

Plate tectonic reconstructions and paleo-geographic maps of the central and north Atlantic oceans

Final report (February 28, 2011)

by Jean-Claude Sibuet¹, Stéphane Rouzo² and Shiri Srivastava³

¹Association Biogéosciences, 44 rue du Cloître, 29280 Plouzané, France;

jean.claude.sibuet@gmail.com

²SRC, 6 rue des Mouettes, 29280 Plouzané, France; srouzo@libertysurf.fr

³Geological Survey of Canada, Bedford Institute of Oceanography, P. O. Box 1006, Dartmouth, N.S., Canada, B2Y4A2; shirisrivastava@eastlink.ca

Objective

Update the plate kinematic reconstructions of the central and north Atlantic oceans, in order to better understand the nature and timing of rifting of Nova Scotia and Morocco conjugate continental margins and provide a series of paleo-geographic maps for seven geological time slices. This is part of the Nova Scotia Play Fairway Analysis “Plate Tectonics” Special Project.

Plan

We propose to:

- 1) Re-examine the interpretation of the velocity structure of the SISMAR04 wide-angle reflection and refraction line by using a more conservative approach with respect to the new trend of the East Coast Magnetic Anomaly (ECMA) and West African Coast Magnetic Anomaly (WACMA).
- 1) Examine the Fugro magnetic data acquired in the area where the ECMA vanishes and determine the potential northern prolongation of the ECMA. Update the trend of the WACMA from a recent compilations of the Bedford Institute of Oceanography (BIO). Compare the shapes of the ECMA and WACMA magnetic lineations.
- 2) Test available and/or determine poles and angles of rotation of the plates for the time of emplacement of significant magnetic anomalies, including ECMA and WACMA.
- 2) Review the timing of ECMA emplacement.
- 4) Provide paleo-geographic reconstructions of the central and north Atlantic oceans for the seven time slices defined below.
- 5) Integrate these results with the recent work undertaken on the Newfoundland/Iberia margins.

Deliverables

Structural elements and outline palaeogeography maps for the following seven time slices:

- 1) Late Triassic - Pre-rift configuration (Norian/Rhaetian limit, about 203 Ma),
- 2) Early Jurassic - end of rifting (after CAMP and salt deposition) (ECMA/WACMA fit, Sinemurian/Pliensbachian limit, 190 Ma),
- 3) Middle Jurassic (BSMA, Middle Bajocian, 170 Ma),
- 4) Late Jurassic (M22, Tithonian, 150 Ma),
- 5) Early Cretaceous (M11, Valanginian, 136 Ma),
- 6) Middle Cretaceous (M0, Late Barremian/Early Aptian, 125 Ma),
- 7) Late Cretaceous (C34, Santonian, 83.5 Ma).

In this study we have adopted the Ogg et al. (2008) geologic time scale.

1. Re-interpretation of OETR2009 and SISMAR04 wide-angle reflection and refraction data

The re-interpretation of SISMAR04 wide-angle reflection and refraction line located in Figure 1 was presented in the SISMAR final report (31 July 2009). The proposed interpretation of the velocity structure, which was determined by using the Korenaga code, was influenced both by the Contrucci et al. (2004) interpretation (Figure 2a) and by the Maillard et al. (2006) interpretation of SISMAR MCS lines (Figure 3). Between OBS07 and 11 along SISMAR04 line, the upper crustal landward reflectors of Contrucci et al. (2004) are dipping eastward (Figure 2a), following the Maillard et al. (2006) interpretation of MCS lines SISMAR04 and 10. The NE-SW oriented SISMAR10 MCS line cuts across the S1 anomaly in the south and SISMAR04 line in the north, in the vicinity of OBS09 (Figure 1). Maillard et al. (2006) identified a landward dipping reflector (LDR) on SISMAR10 and 09, but not on profiles SISMAR04 and 05, where only faint landward dipping crustal reflections are identified. Maillard et al. (2006) interpret the landward dipping reflectors as a detachment surface which was active during the rifting period (Figure 3). Figure 4 shows the SISMAR04-SMART01 2-D model of Maillard et al. (2006), which does not consist of true conjugate profiles, as the two conjugate sections are ~170 km apart. Assuming the lack of conjugacy is overcome by the 2 dimensionality of the conjugate margins, they proposed a rifting episode in two stages: a widespread crustal extensional stage followed by the exhumation of the lower continental crust and mantle through the play of a large detachment surface as suggested on other margins by Whitmarsh et al. (2001). However, the crucial ingredient of the model (the detachment fault) is not representative of the two conjugate sections as it is located in between and does not correspond to what is observed on the SISMAR04 profile. We will look in detail both the interpretation of the SISMAR MCS lines and the new interpretation of the SISMAR04 velocity structure, to demonstrate that the detachment model cannot apply to the SISMAR04 profile.

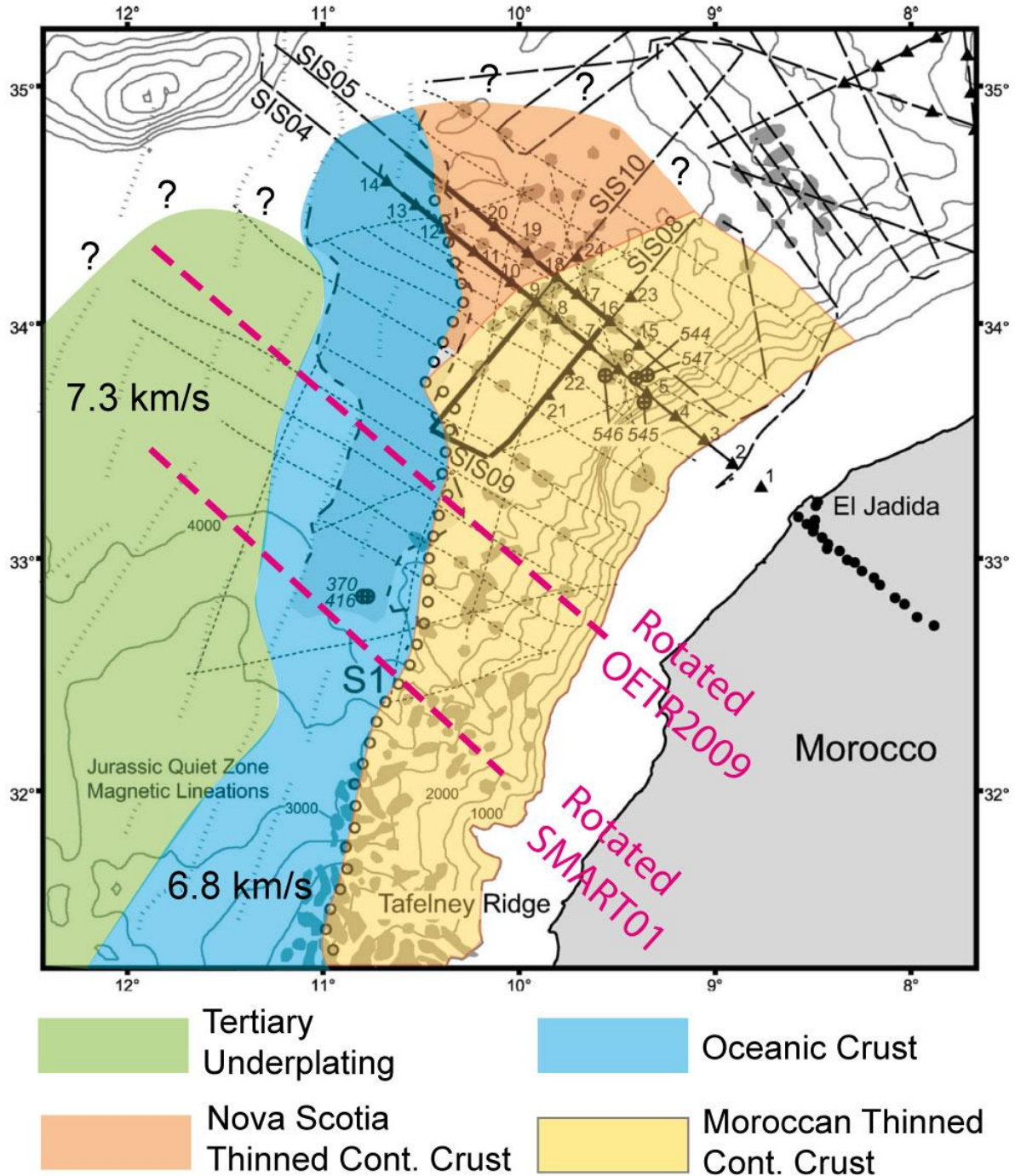


Figure 1: Location of MCS and wide-angle reflection and refraction SISMAR lines shown in this study. Open dots underline the S1 magnetic lineation. Salt diapirs (small gray polygons) are mostly located landward of S1 (Maillard et al., 2006). DSDP holes are indicated. In light green, the extent of unusually high 7 km/s + underplated crust emplaced during Tertiary and in light blue the oceanic crust determined from sonobuoy data (Holik et al., 1991). In light yellow the Moroccan thinned continental crust and in light orange the portion of transferred Nova Scotia thinned continental crust. The limit between the light orange and yellow thinned continental crusts is the western extent of the Moroccan thinned continental crust; it is constrained by the SISMAR MCS and refraction data.

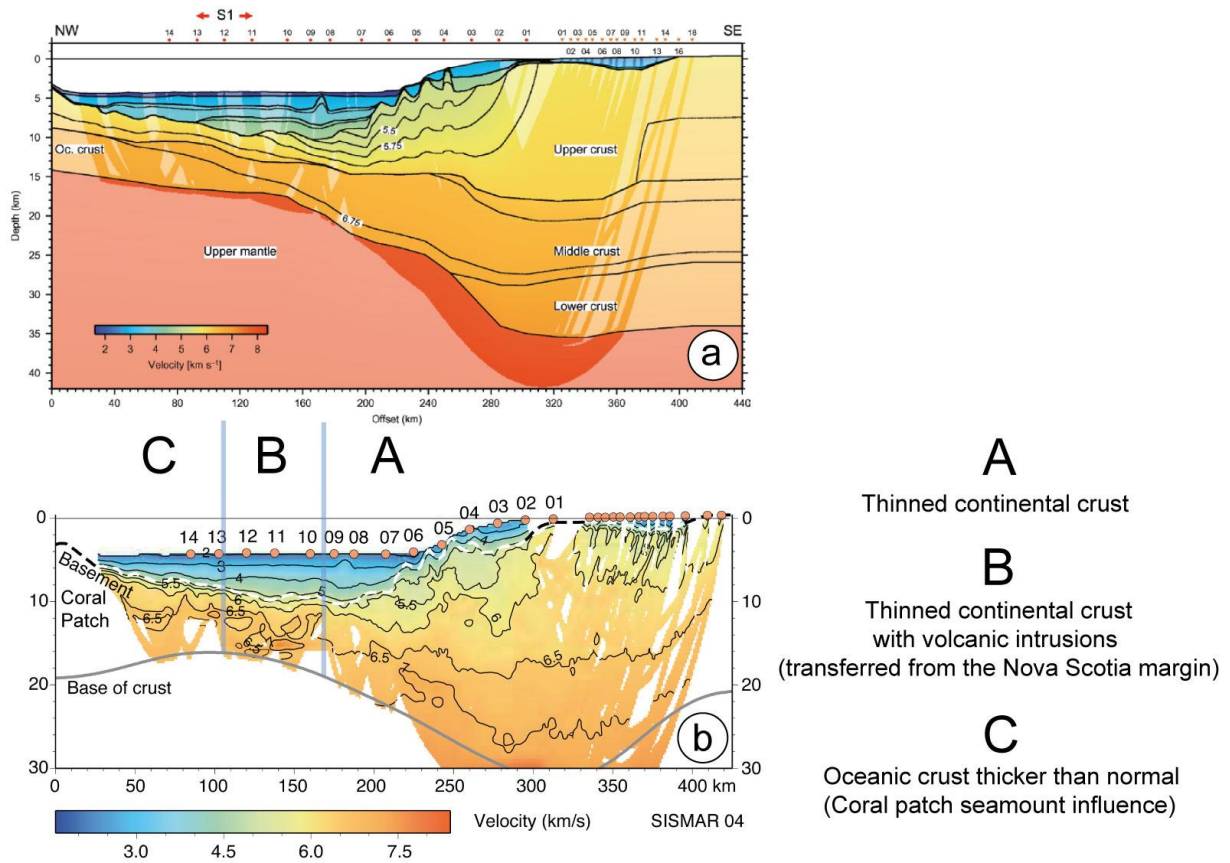


Figure 2: Comparison between the Contrucci et al. (2004) velocity model (a) and the tomographic model (b), with similar color scale and iso-value contours for proper comparison. Note that between OBH09 and OBH10, there is a sharp boundary between the Moroccan thinned continental crust and a thinned continental crust intruded by volcanics that we interpret as transferred from the Nova Scotia margin. See discussion in sections 1.2 and 2.3.

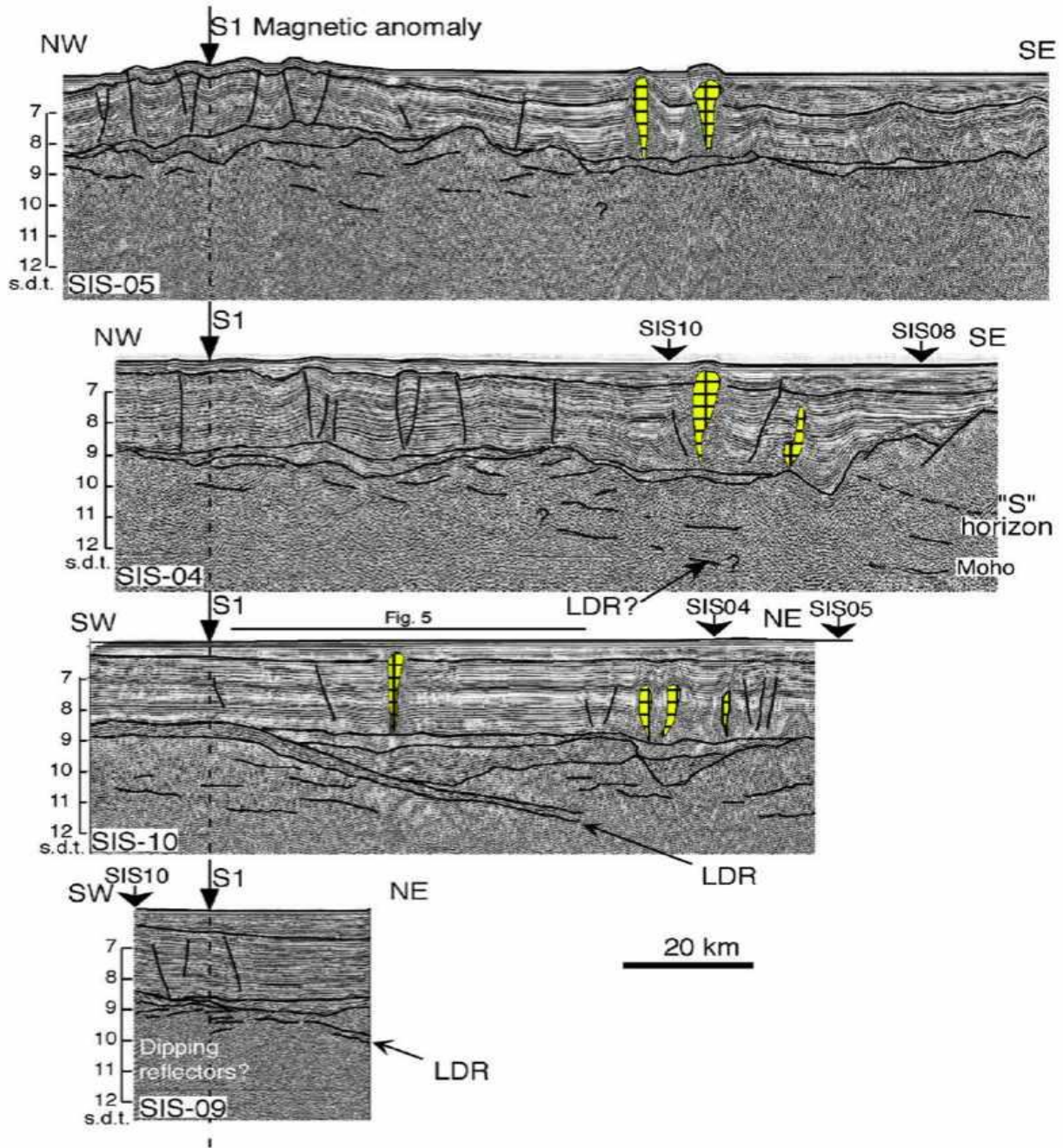


Figure 3: The four SISMAR MCS profiles are aligned with respect to S1 located in Figure 1. The landward dipping reflector (LDR) is identified on SISMAR10 and 09, but not on profiles SISMAR04 and 05 where Maillard et al. (2006) have identified discontinued crustal reflections dipping landward. Above the LDR, the layered unit (LU) is ~0.5 second thick.

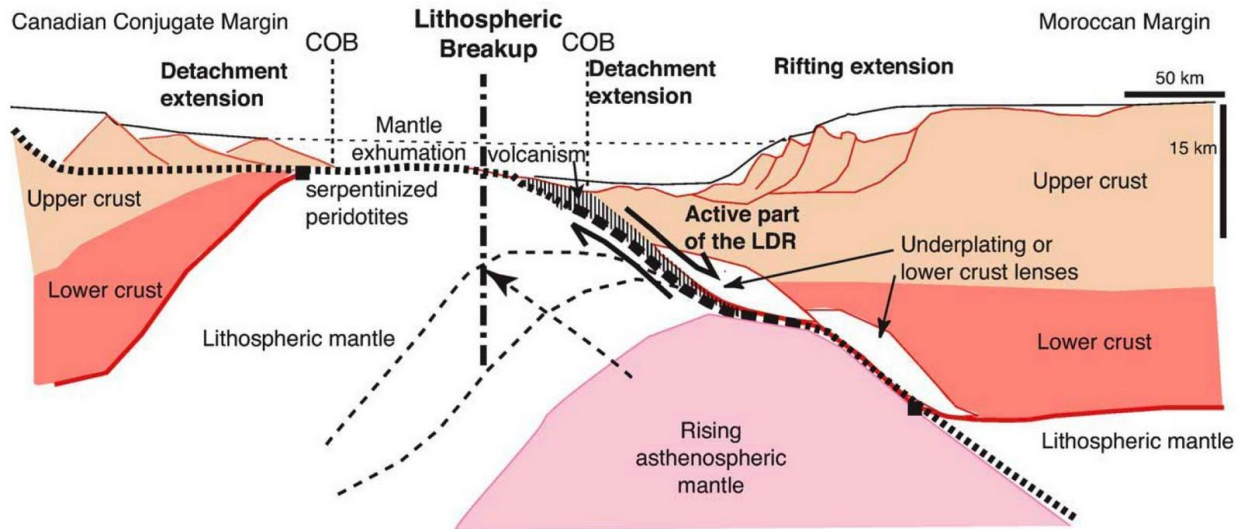


Figure 4: 2-D model of the conjugate margins of the Morocco and Nova Scotia margins based on SISMAR04 and SMART01 lines and proposed by Maillard et al. (2006).

1.1. Re-interpretation of SISMAR MCS profiles

Figure 5 shows a detailed portion of MCS seismic profile SISMAR10 interpreted by Maillard et al. (2006) in Figure 3. In our interpretation, the landward dipping reflectors (noted LDR by Maillard et al. (2006)) only extends 30 km landward from the emergence point of the LDR compared to 45 km in Figure 3. From MCS data, it is impossible to detect any seismic structure in the crust above the detachment. S1 anomaly is located about 25 km oceanward of the emergence point of the LDR. The thickness of the transparent layer beneath both the LDR and the transitional crust is 2-2.2 seconds twt, i.e. about 7 km. It suggests that the portion of crust located between S1 and the emergence point of the LDR might be composed of transitional crust, possibly exhumed mantle from beneath the thinned continental crust, as proposed by Maillard et al. (2006).

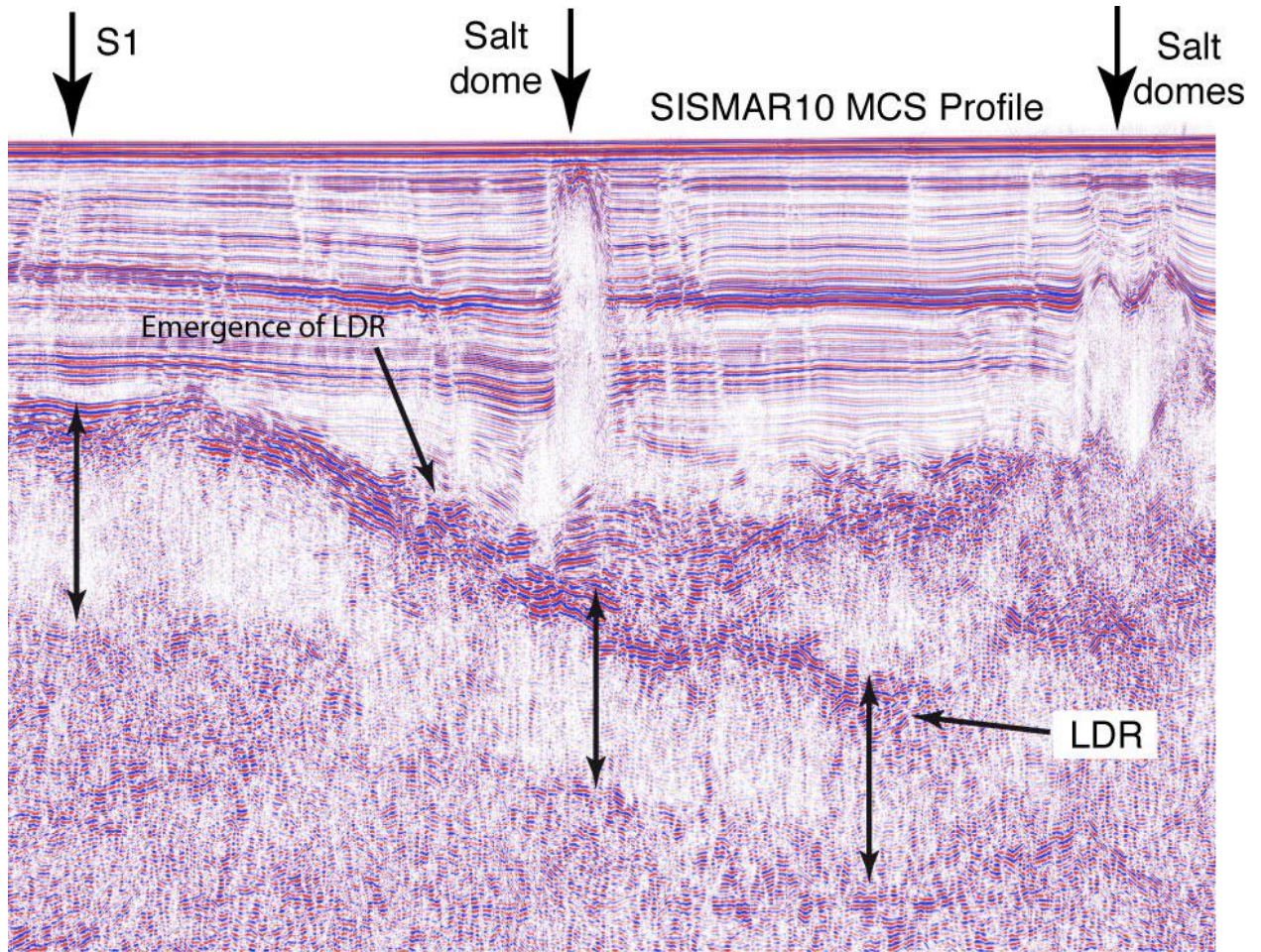


Figure 5: Detailed portion of MCS seismic profile SISMAR10 (J. Perrot, personal communication, 2010). Note that the landward dipping reflectors (noted LDR by Maillard et al. (2006) in Figure 3) only extends 30 km landward from the emergence point of the LDR compared with 45 km in Figure 3. S1 is located about 25 km oceanward of the emergence point of the LDR. The thickness of the transparent layer beneath the LDR and the transitional crust is 2-2.2 seconds twt, i.e. about 7 km (exhumed lower crust or mantle?).

Figure 6 shows a detailed portion of MCS seismic profile SISMAR04 interpreted by Maillard et al. (2006) in Figure 3. We do not see any clear landward dipping crustal reflectors as interpreted in Figure 3, except perhaps where “LDR?” is mentioned. However, the basement is very hummocky and numerous reflections are observed beneath it, suggesting that “LDR?” might have an other meaning. In addition, we do not identify a transparent crustal layer as observed in SISMAR10 (Figure 5), suggesting that the nature of the crust is different in these two sections located 60 km apart and that the supposed cylindrical symmetry of the margins is not confirmed. However, from MCS data alone we cannot clearly establish the nature of the crust. The indications concerning the nature of the crust mentioned above the seafloor will be discussed later on in sections 1.2 and 2.3.

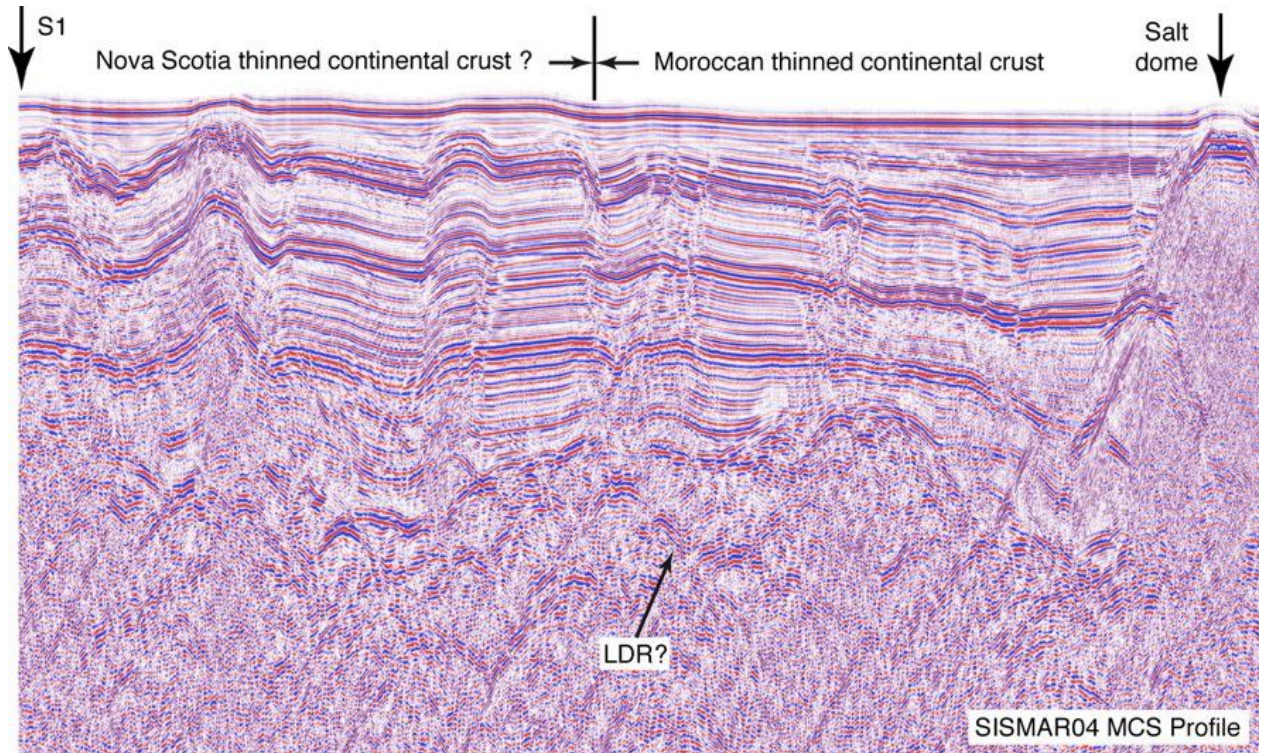


Figure 6: Detailed portion of MCS profile SISMAR04 (J. Perrot, personal communication, 2010). Note that the landward dipping reflectors (noted LDR? by Maillard et al. (2006) in Figure 3) are hypothetical. There is no clear evidence of the presence of LDRs on MCS SISMAR04 profile. Note also that the seismic character of the crust is different from the one of the crust in SISMAR10 (Figure 5).

1.2. Re-interpretation of SISMAR04 wide-angle reflection and refraction profile

Figure 7 shows the 1-D vertical velocity profiles extracted below instruments 08 to 14. When compared to trial-and-error Zelt inferred velocity profiles (Figure 7a), the tomographic-based velocity profiles (Figure 7b and c) are quite rough and sometimes spiky. It actually reflects the difference between what is required in the velocity model (tomographic approach) and what is required and interpreted by a geologist eye (modeling by hand).

The broken line aspect of velocity profiles of Figure 7a reflects the paradigm on which Zelt code *Rayinvr* is based (linearly varying velocities within layers and strong velocity jumps at layers interfaces) and the grid mesh used in the tomographic experiment (velocities are continuously varying) (Figures 7b and c). For example, the ~ 7.54 km/s spike of the purple curve (OBH11, Figure 7b) observed at $z = 5$ km corresponds to the positive velocity anomaly observed in the model (Figure 2b).

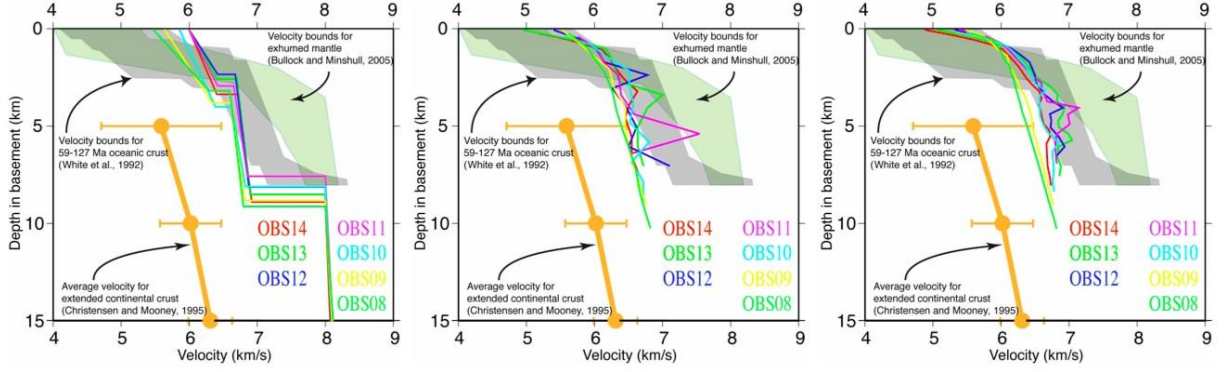
As OBH08 and 09 are clearly outside the oceanic crust envelopes on all the three graphs of Figure 8 and regularly increasing in velocity with depth (Figures 7b and c), OBH08 and 09 are located above thinned continental crust, even if the crust between 170 and 210 km is sparsely covered, implying a lower resolution. Thus, the continental crust and thinned continental crust (domain A, Figure 2b) extends from OBH01 to OBH09 ($x > 175$ km).

Localized maximum velocities of 7+ km/s (7.4 and 7.1 km/s) are observed beneath OBH11 (Figures 7b and c respectively) at 14-15 km depth (Figure 2b), 7 and 6.9 km/s beneath OBH13 (Figures 7b and c respectively) and 6.6 and 6.8 km/s beneath OBH14 (Figures 7b and c respectively), showing

that these velocities slightly decrease westward from OBH11 to OBH14 (domain B). Compared to the envelopes of 60-to-130 Ma oceanic crust (White et al., 1992) and exhumed mantle (Bullock and Minshull, 2005), Domain C is probably composed of oceanic crust abnormally thick to the west (Figure 2b). Contrucci et al. (2004) also interpret crustal velocities below OBH13 and 14 as “more” typical of oceanic crust even if the crust beneath OBH13 and 14 is thicker than normal and velocities are either on the extreme left-hand side of the oceanic crust envelope or lower than normal at depths deeper than 5 km below basement. As OBH13 and OBH14 are located on the flank of Coral Patch seamount (Domain C), the crust beneath these two OBHs might be related to the oceanic nature of the abnormally thick Coral Patch crust. If this is true, the westernmost extremity of the SISMAR04 profile would not be similar to the conjugate portion of OETR2009 Profile.

A region of thin crust approximately 60 km wide (Domain B) marks the transition from thinned continental crust (Domain A) to abnormally thick oceanic crust (Domain C). Domain B only exhibits a few anomalously high P-wave velocities, which suggests that this domain cannot be simply associated to the serpentinized upper mantle typically found on magma-poor volcanic margins and to the high velocity body found on OETR2009 Profile (C. Keen, personal communication, 2010). It could not be oceanic material because crustal velocities in the lower part of the crust are outside the White et al. (1992) oceanic bounds (Figure 7b and c). However, this material could represent a thinned, and possibly broken up, continental crust intruded by partial melt (CAMP volcanism?). The presence of autochthonous salt, not on SISMAR04 profile but in its immediate distal vicinity (Figure 1) suggests a shallow marine salt deposition in favor of the presence of thinned continental crust. In addition, it is not excluded that some underplating might have occurred during rifting to take into account the 7+ km/s high velocities observed at the base of the crust. Indeed, we will see later on salt reconstructions at ECMA (190 Ma) and BSMA (170 Ma) times that Domain B might correspond to a portion of Nova Scotia thinned continental crust transferred on the Meseta plate 190 My ago and presently adjacent to the thinned Moroccan continental crust (section 2.3).

To conclude, the SISMAR04 line can be considered as representative of the Moroccan margin only for the portion of margin located east of OBH09-10, comprising the Moroccan continental and thinned continental crusts. The OBH10-12 portion of the profile (Domain B) probably consists of a portion of Nova Scotia thinned continental crust intruded by volcanics and transferred to the Moroccan side at the time of ECMA emplacement (190 Ma) (Figure 2b). The OBH13-14 portion of the profile and westward (Domain C) consists of an abnormally thick oceanic crust.



a) SISMAR velocity model for the transitional crust (Zelt code) b) SISMAR velocity model for the transitional crust (Korenaga code) c) SISMAR velocity model for the transitional crust (Korenaga code) (detailed model)

Figure 7: 1-D vertical velocity profiles below each OBH (continuous curves of various colors) when using the Zelt and Korenaga codes: close-up for vertical profiles OBH08 to OBH14. The vertical axis indicates the depth below the top-basement, defined on the coincident MCS profile. The thick orange line with error bars is the average velocity profile in extended continental crust (Christensen et Mooney, 1995). The gray and green shaded areas are the envelopes of 1-D velocity profiles in 60-to-130 Ma oceanic crust (White et al., 1992) and in exhumed mantle (Bullock and Minshull, 2005), respectively.

1.3. Nature of the crust west of S1 anomaly

Using numerous sonobuoy data, Holik et al. (1991) identified an area roughly corresponding to the Canary swell, featuring high lower crustal velocities (7.1-7.4 km/s) (Figure 8). The thickness of the high lower crustal body is 4-5 km (Holik et al., 1991) and is interpreted as resulting from Tertiary underplating linked to the Canary thermal anomaly and clearly not formed during the rifting of Morocco and Nova Scotia continental margins. Holik et al. (1991) data also show that outside of the 7.3 km/s area contoured in Figure 8, and in particular between the Canary swell and S1 anomaly, lower crustal 6.8 km/s velocities are observed south of 34°N, along a ~70-km wide stripe. As these sonobuoy data are the only available refraction data in the area south of SISMAR04 line, we have displayed them in function of the depth below basement (Figure 9). All the velocities are within the White et al. (1992) bounds of oceanic crust, clearly suggesting that the crust located westward of S1 anomaly is oceanic, with a mean thickness of 6.5-7 km. Thus, west of S1 in the south and west of S1old in the north, the nature of the crust is oceanic, including north of 34°N, on SISMAR04 line where the oceanic crust thickens in the vicinity of Coral Patch Seamount. The seafloor spreading rate (between ECMA and Blake Spur magnetic anomaly (BSMA)) is low, about 1.6 cm/yr full rate (Labails et al., 2010). Typical oceanic crust may be emplaced at such low spreading rate.

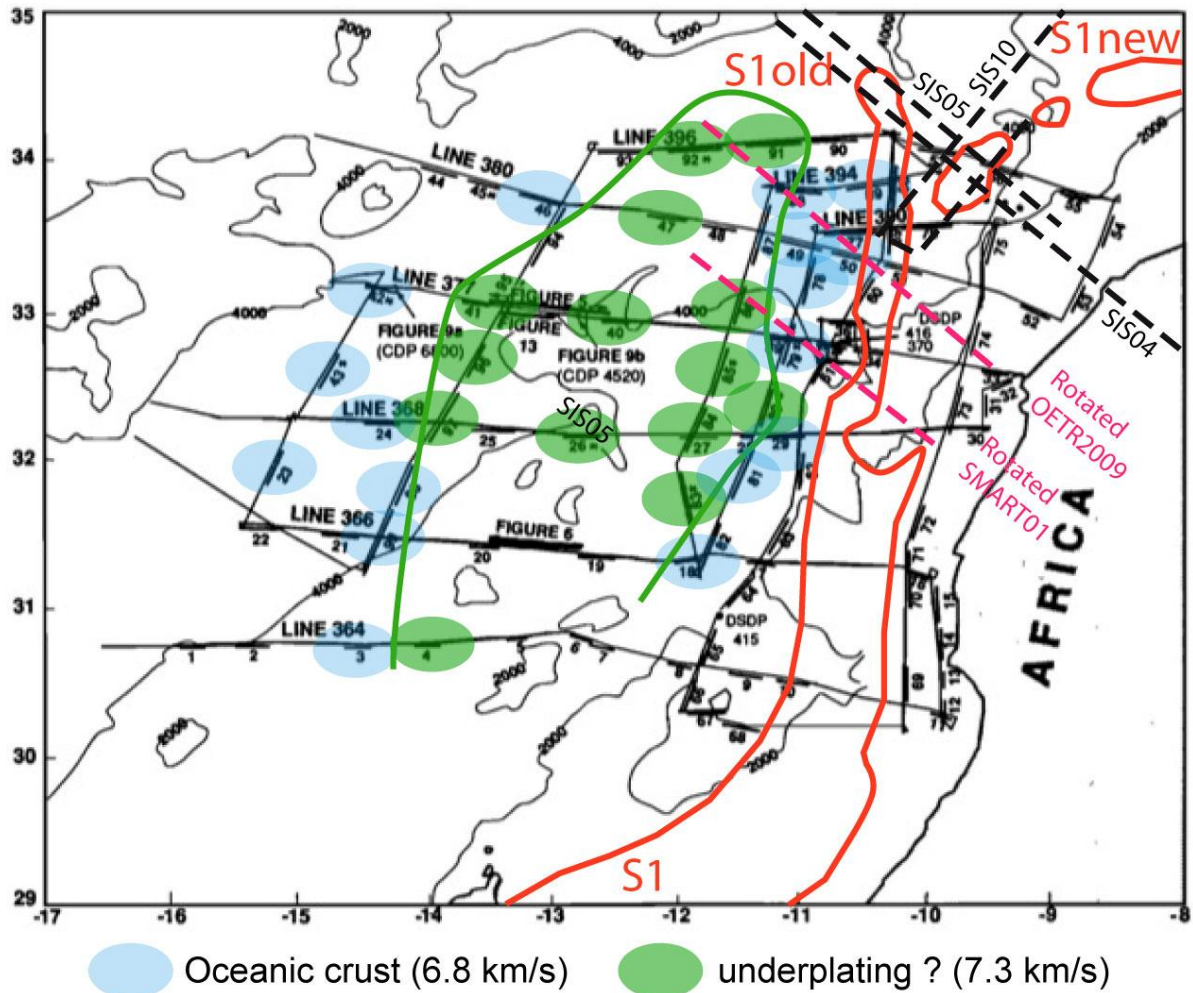


Figure 8: Location of sonobuoys used in Holik et al. (1991) study. In light green and light blue, sonobuoys where 7.3 and 6.8 km/s lower crustal velocities have been identified, respectively.

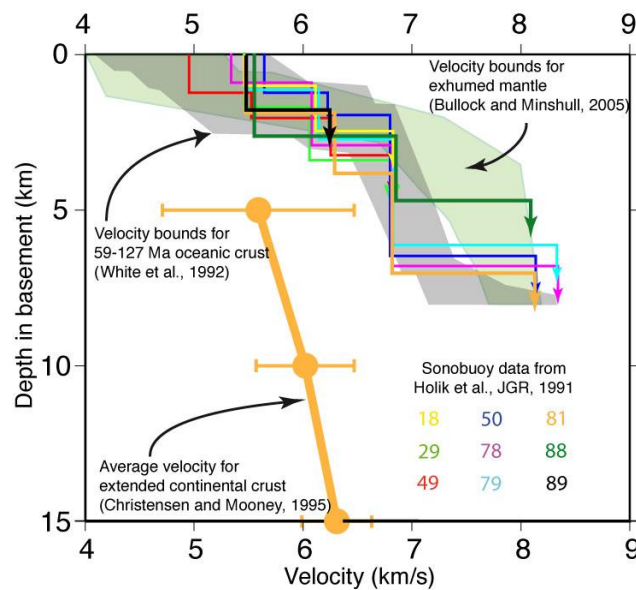


Figure 9: 1-D vertical velocity profiles of Holik et al. (1991) in the area located between S1/S1old anomaly and the Tertiary Canary swell where underplating has been evidenced. The vertical axis indicates the depth below the top-basement, defined on the MCS profiles. The thick orange line with error bars is the average velocity profile in extended continental crust (Christensen et Mooney, 1995). The gray and green shaded areas are the envelopes of 1-D velocity profiles in 60-to-130 Ma oceanic crust (White et al., 1992) and in exhumed mantle (Bullock and Minshull, 2005), respectively.

On Profile SISMAR09, some dubious dipping diffractive reflectors have been identified by Maillard et al. (2006) oceanwards of the LDR emergence point and interpreted as seaward dipping reflectors of limited extent (SDR's). However, they are located westward of the continental crust domain, clearly on top of the oceanic crust. The other occurrence of published dipping reflectors is offshore Tafelney Ridge (Roeser et al., 2002), close to line 377 (Figures 1 and 8) and westward of S1 anomaly also on top of the oceanic crust. Roeser et al. (2002) also noticed that within this ~70-km stripe of oceanic crust, dipping reflectors are mostly dipping seaward in the eastern part of the stripe, more or less horizontal in the central part of the stripe and mostly dipping landward in the western part of the stripe. This is a common feature observed in the oldest oceanic crusts located close to the base of continental margins (e. g. in the northern Bay of Biscay, Thinon et al. (2003)). In general, the basement is rather flat, suggesting the emplacement of excessive magma supply or superposed flood basalts which may explain the occurrence of flat or dipping reflectors. These dipping reflectors are all observed on top of typical oceanic crust and cannot be considered as SDR's typically formed on volcanic margins. We will see in section 1.4 that the age of the oldest oceanic crust is late Toarcian (177 Ma), much younger than the end of the rifting episode (190 Ma).

The existence of this stripe of oceanic crust adjacent to the thinned continental crust where autochthonous salt is observed also raises the question of interpretation of the LDR reflector identified by Maillard et al. (2006) on SISMAR10 MCS line (Figures 3 and 5).

1.4. Composite SISMAR04 and OETR2009 wide-angle reflection and refraction profile

Figure 10 shows that the lack of conjugacy between SISMAR04 and OETR2009 and between SISMAR04 and SMART01 lines is about 80 and 160 km, respectively. Maillard et al. (2006) have produced a composite cross-section of the Nova Scotia and Morocco margins by using arbitrarily the informations of MCS SISMAR10, introducing a bias in the model of conjugate margins (Figure 4). We have demonstrated that there is no clear LDR on SISMAR04 (Figure 6). Consequently, a composite model of conjugate margins using Line SISMAR04 on the Moroccan side cannot include a detachment surface. However, a composite model of conjugate margins located in the vicinity of the green profile (Figure 10) and using a profile where the emergence of the LDR is seen (e.g. Profile SIMAR10) may include a detachment surface. Such a recorded profile perpendicular to the margin does not exist and it is difficult to use SISMAR10, as this profile is close to be along strike and is perpendicular to OETR2009 and SMART01 lines.

This discussion helps to understand that: 1) Conjugate profiles which includes SISMAR04 and an hypothetical conjugate NS line located 80 km NE of OETR2009 line (blue line in Figure 9) would not display a detachment surface; 2) Conjugate lines crossing the area of the emergence of the LDR on SIMAR10 (green line) would display a detachment surface, but they don't exist. The implication of this discussion is that areas where a detachment surface is observed are generally restricted in space. For example, there is a several tens of km parallel-to-the-margin detachment surface identified beneath

Galicia Bank which does not exist beneath the Iberia Abyssal Plain margin. Similarly, the scale of mullions or megamullions in the oceanic crust (which are similar features in the oceanic crust) is also several tens of km parallel to the rift. However, generally speaking, areas where detachment surfaces exist are far less than areas without detachment surfaces. Thus, it seems difficult to identify an area where a detachment fault exists over more than a few tens of km. In addition, for the Galicia Bank/SE Flemish Cap conjugate margins where detachment faults have been identified on both margins, leading to the apparent contradiction that both margins seem to be upper plates to a detachment fault, Ranero and Pérez-Gussinyé (2010) have proposed an explanation which does not require the existence of an active detachment fault and is compatible with Andersonian mechanics allowing slip until a fault angle of 30° is reached.

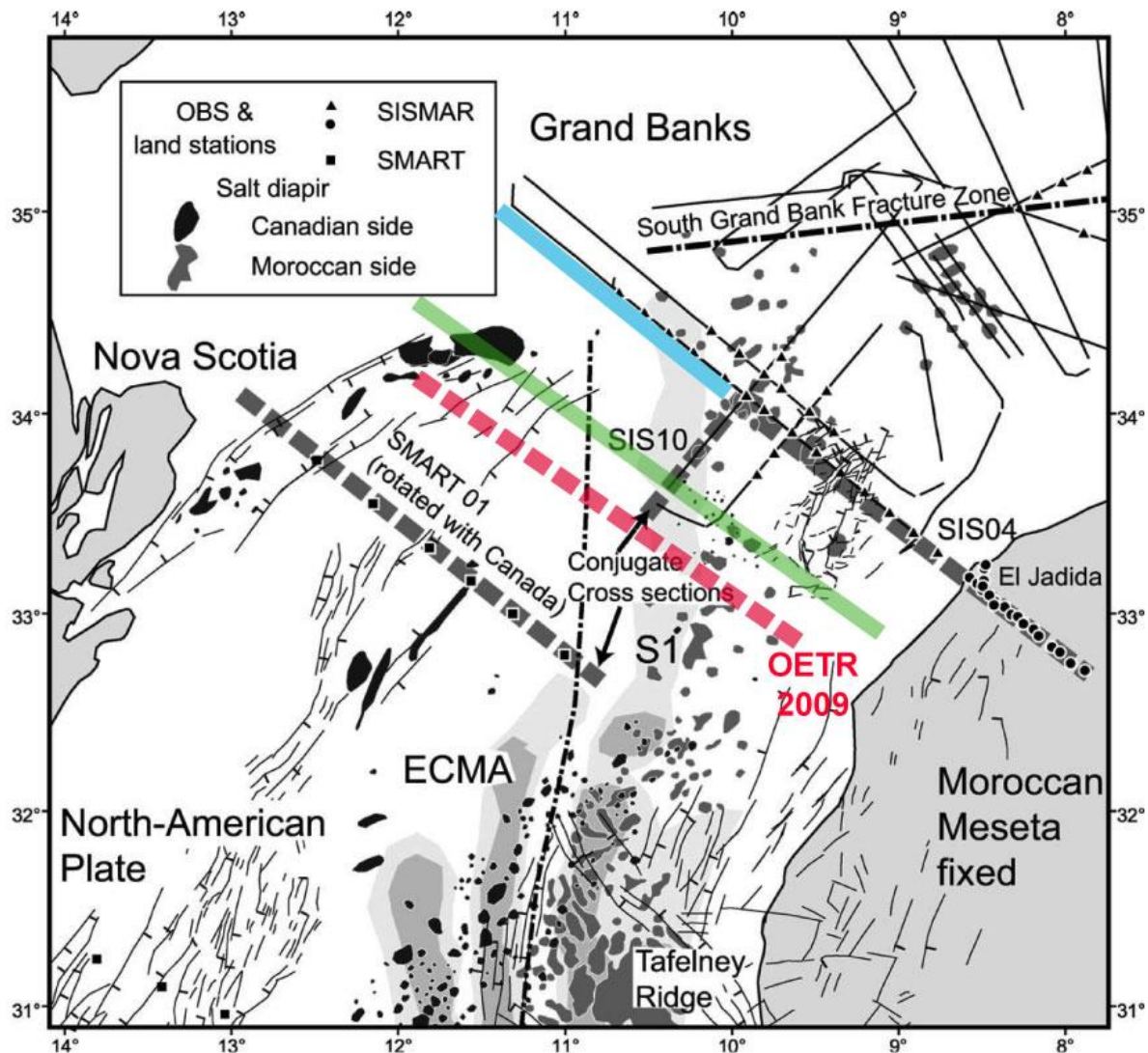


Figure 10: Maillard et al. (2006) reconstruction at the time of juxtaposition of the magnetic anomalies S1 and ECMA. The line of breakup is shown as a stippled-dashed line. SISMAR04 and SMART01 lines

(black squares) and OETR2009 line (red squares) are shown. The composite profile shown in Figure 4 is build on SISMAR10. Thin continuous lines represent faults on each margin.

Figure 11 shows the location of the four available wide-angle and refraction seismic profiles acquired off Nova Scotia. Lines OETR2009, SMART01 and SMART02 display similar high velocity bodies located at the base of the crust (Figure 12). The green line (Figure 10) corresponds to the oceanward limit of the thinned continental crust and the landward boundary of the high velocity body. It follows the oceanward boundary of the ECMA. This oceanward limit of the thinned continental crust is also evidenced on coincident MCS lines. Though magnetic forward modelling shows that ECMA might be associated with a thinned volcanic layer located in the upper part of the layer overlying the high velocity body and also landward of it (S. Delher, personal communication, 2010), we cannot exclude that the magnetic signal might include an edge effect due to the juxtaposition of a magnetized serpentized body with a non-magnetic continental crust. Only inversion of magnetic data (Euler deconvolution) could be able to decipher between these two possibilities. In any case, the thin volcanic layer might be interpreted as a basaltic and gabbroic layer formed by decompression melting as observed in the drill sites off Iberia and Newfoundland (Tucholke and Sibuet, 2007). Thus, we have rather the characteristics of an amagmatic continental margin, even if a few CAMP volcanic features have been emplaced during rifting, some of them being intruded through the contemporaneous salt layer.

Line SMART03 and the coincident MCS profile show the presence of a significant amount of SDRs (associated with the strong portion of ECMA), showing that this portion of margin is magmatic. The boundary between the magmatic and amagmatic segments of continental margins is located somewhere in between SMART02 and SMART03 lines (Lau et al., 2010) (Figure 11).

On the Moroccan side, the identification of volcanic material within the thinned continental crust always located eastward of S1/S1old anomaly is poor. Although Maillard et al. (2006) suggest by forward magnetic modelling that some volcanics might have been emplaced along the LDR of SISMAR10 line, there is no clear seismic image of these volcanic bodies on available MCS data.

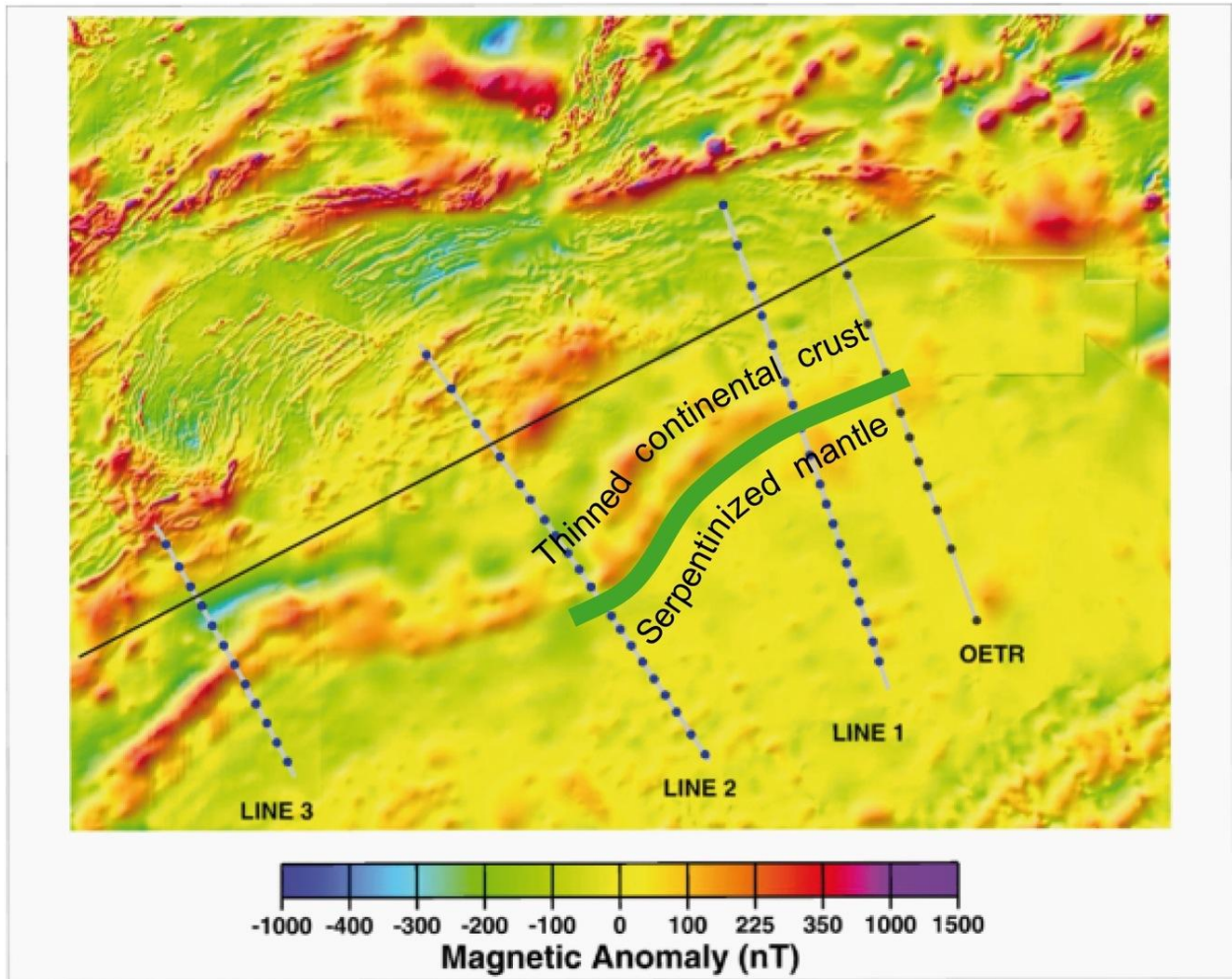


Figure 11: Location of the four wide-angle reflection and refraction lines on the magnetic anomaly map of Dehler (2010). OETR: OETR2009 line; Line 1: SMART01 Line; Line 2: SMART02 Line; Line 3: SMART03 Line. The green continuous line following the oceanward boundary of the ECMA also marks the seaward limit of the thinned continental crust and the landward limit of the lower crustal high velocity body.

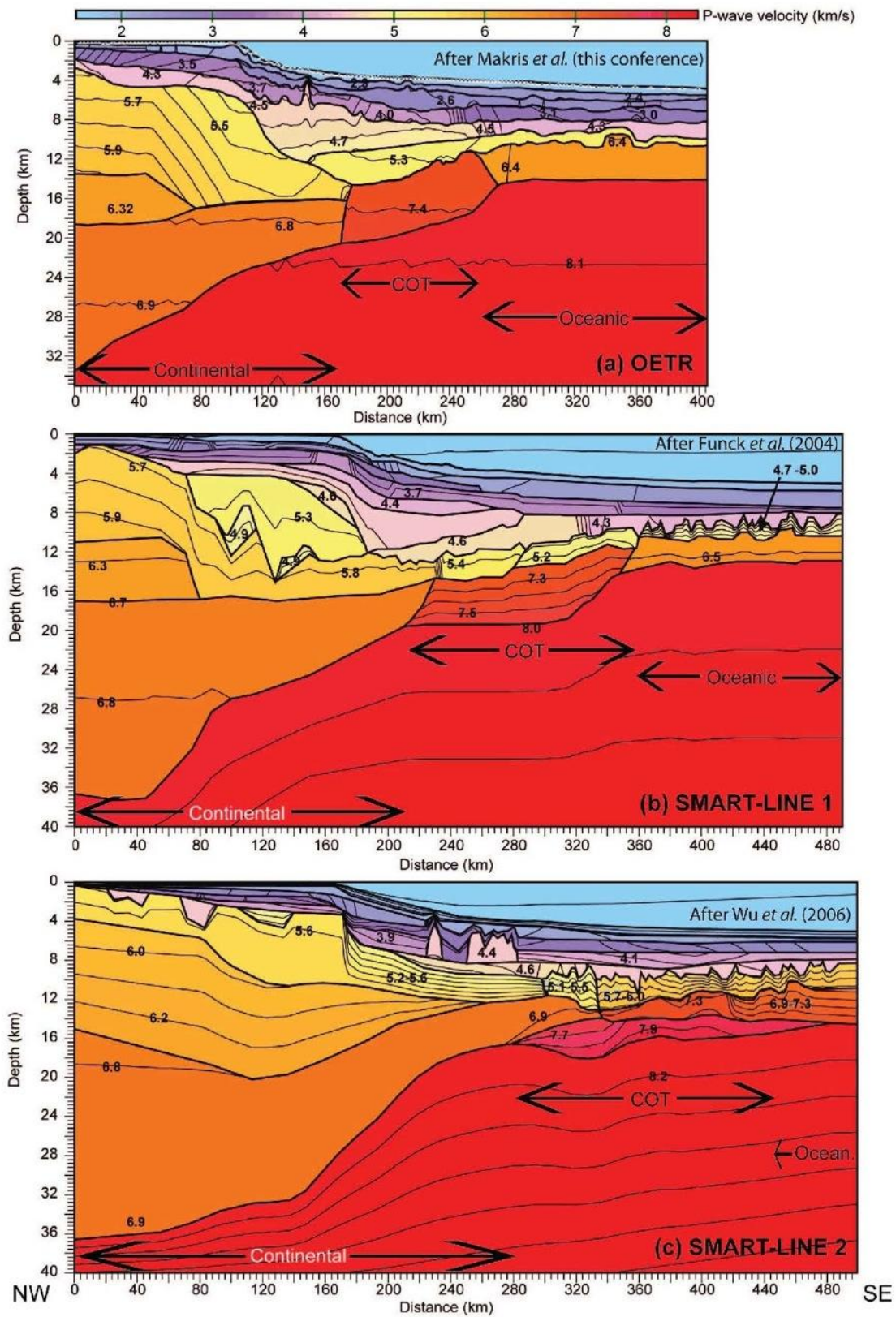
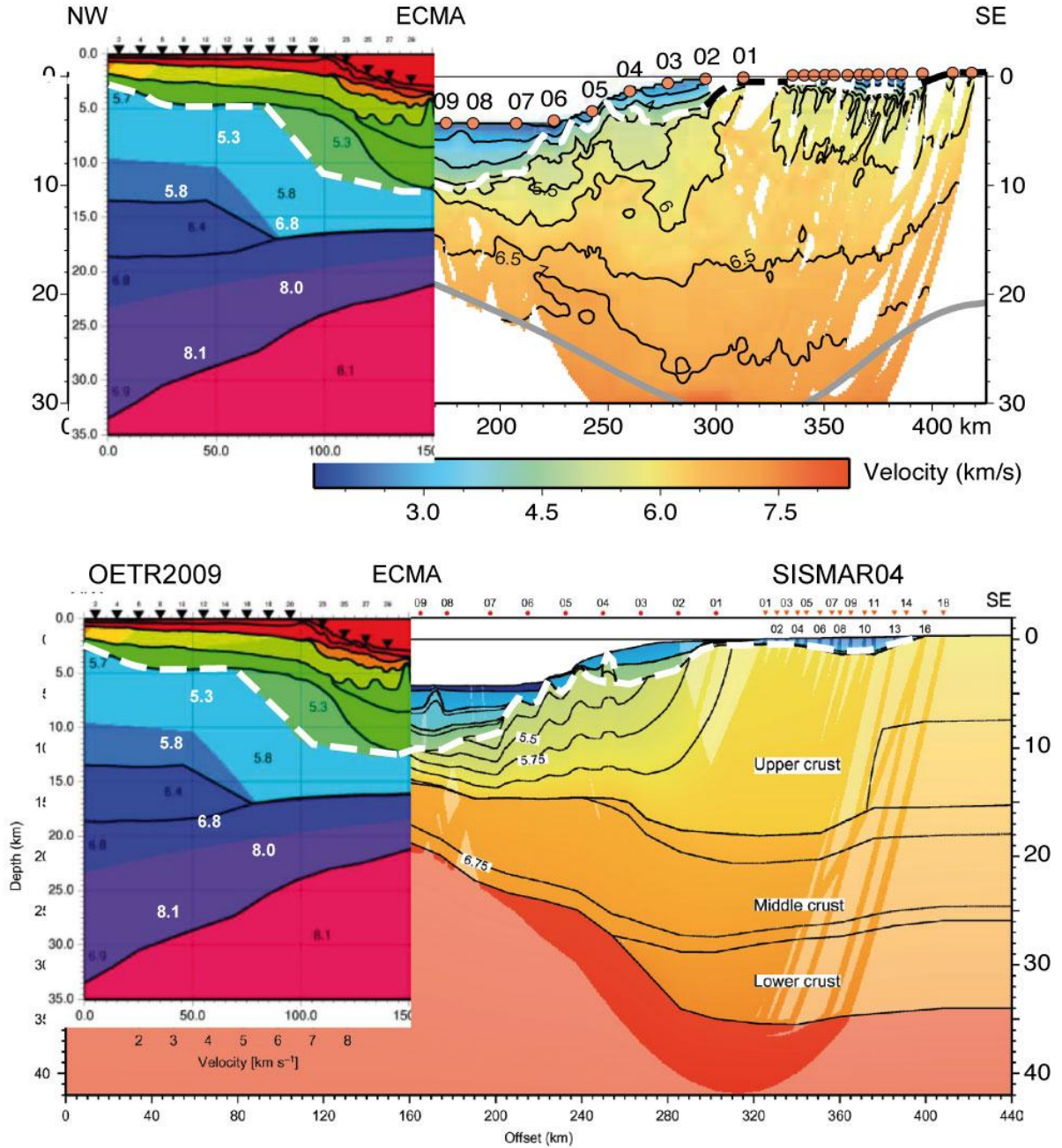


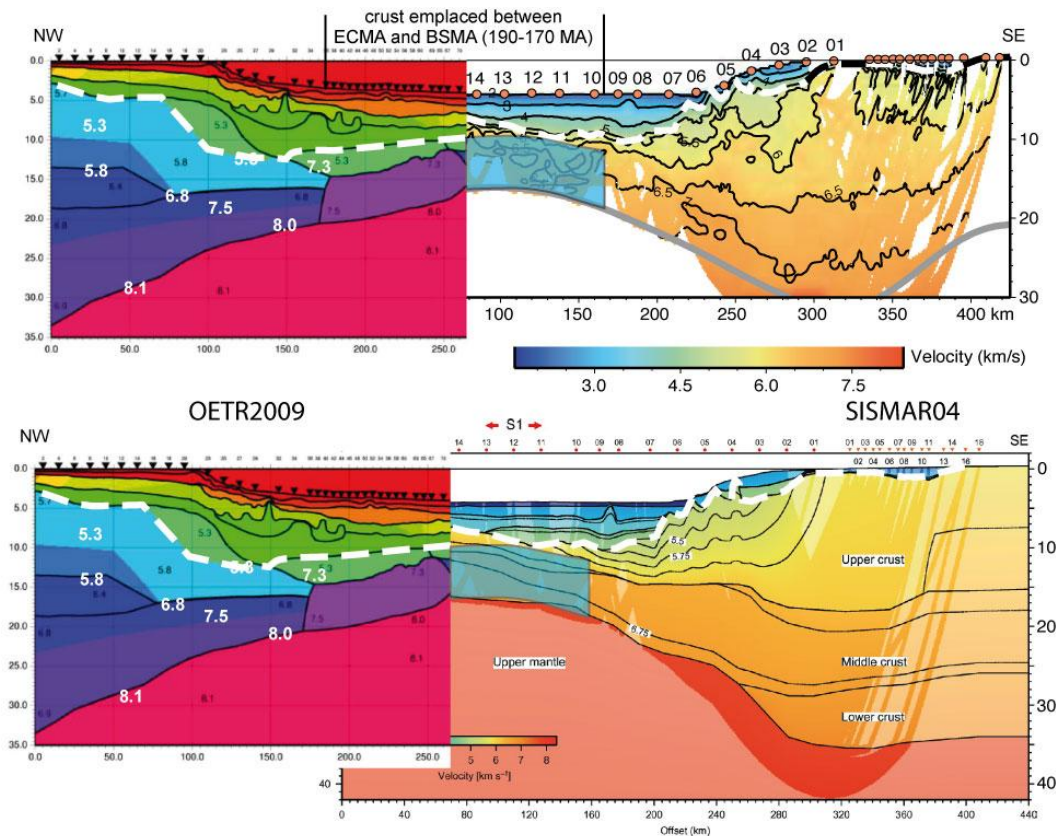
Figure 12: *P*-wave velocity models of OETR2009, SMART01 and SMART02 lines across the NE Nova Scotia margin (locations of lines in Figure 11) (Lau et al., 2010).



OETR2009 and SISMAR04 conjugate profiles at 190 Ma (ECMA): juxtaposition of thinned continental crusts

Figure 13: Conjugate velocity profiles SISMAR04 and OETR2009 with the two types of interpretations (Zelt (bottom) and Korenaga (top) codes) at the time of emplacement of ECMA (190 Ma). Preliminary interpretation of Profile OETR2009 from Makris et al. (2010). As the sediment thickness is double on the Nova Scotia side compared to the Moroccan side, Profile OETR2009 has been moved upwards in order to show crustal coincidence.

Figure 13 shows the OETR2009 and SISMAR04 conjugate profiles at the end of the rifting episode (ECMA, 190 Ma). Figure 14 shows the same OETR2009 and SISMAR04 conjugate profiles at 170 Ma (Bajocian). In light blue we have superposed a 6.5-7 km thick oceanic crust identified further south on Holik et al. (1991) data on top of Domain B of SISMAR04 profile interpreted as Nova Scotia thinned continental crust intruded by volcanics with possible underplating (OBH10 to 12) and oceanic crust (OBH13 and 14).



OETR2009 and SISMAR04 conjugate profiles (Early Middle Jurassic)

Figure 14: Conjugate velocity profiles SISMAR04 and OETR2009 with the two types of interpretations (Zelt (bottom) and Korenaga (top) codes) at 170 Ma (Bajocian). Preliminary interpretation of Profile OETR2009 from Makris et al. (2010). Juxtaposition of the high velocity body on the NA side and either the transferred NA thinned continental crust (OBH10 to 12) and oceanic crust further west (OBH13 and 14) (beneath the light blue) or oceanic crust identified further south on Holik et al. (1991) data (in light blue).

Figure 15 is a sketch which summarizes what we know about the two conjugate profiles at 190 Ma (ECMA, Sinemurian/Pliensbachian limit) and 170 Ma (BSMA, Bajocian). The width of the oceanic crust domain (50 km) has been estimated assuming that: i) the domain created in between the thinned continental crusts is 140 km and ii) a half-spreading rate of 0.7 cm/yr between ECMA and BSMA at the latitude of the transect.

The conjugate profiles at 170 Ma are surprising. The Nova Scotia high velocity body is interpreted as a serpentinized mantle capped by a layer of highly serpentinized mantle due to the Fisher-Tropsch reaction (slow sea-water/peridotite reaction creating serpentinite and talc). This interpretation of the high velocity body has been proposed by numerous authors (e.g. Funck et al., 2004 for SMART01; Wu et al., 2006 for SMART02). One of the argument which may contradict this interpretation is that the velocity variation at the Moho location beneath the high velocity body is too weak, considering that it is the same mantle beneath and above the Moho and that serpentinization effect was not able to reach the Moho interface as expansion of the peridotites during the serpentinization process seals the fractures and fluid paths in the rock and thus prevents sea-water from penetrating deeper into the mantle.

At this time it might be worthwhile to consider how much melt could have been generated during rifting using the model of Bown and White (1995), in which the melt is produced by mantle decompression during uniform pure shear extension of continental lithosphere. The stretching factor along the northern Nova Scotia margin is 2 for the whole margin (B. Colletta, personal communication, 2010) but 5 where the continental crust is the thinnest, at the contact with the high velocity body. With the rifting starting at 203 Ma and ending 190 Ma ago, i.e. a 13-My long duration of rifting, according to Bown and White (1995) no melt should be generated with an extension factor of 5 and an asthenosphere potential temperature of 1300°C because the rift duration is sufficient to cool the asthenospheric mantle. However, for an asthenosphere potential temperature of 1350°C, the final melt thickness would be 1.3 km. Thus, the interpretation of the transition zone as serpentinized mantle is consistent with the melt generation model of Bown and White (1995) and the presence of a thin layer of volcanic material as given by the forward magnetic modeling of S. Delher (personal communication, 2010). In addition, the oceanic crust adjacent to the high velocity body is about 4 km thick on both OETR2009 and SMART01 lines, which is in agreement with a slow seafloor spreading and a low asthenosphere potential temperature (Dick et al., 2003), which creates oceanic crust with a thickness of <4 km (e.g., Mohs Ridge (Klingelhoefer et al., 2000), Gakkel Ridge (Jokat et al., 2003), extinct Labrador Sea spreading center (Louden et al., 1996)).

The evidence of SDRs on the Moroccan side is weak, even if a few dipping reflectors are reported in Maillard et al. (2006) and Roeser et al. (2002) and are considered by these authors as able to produce the amplitude of anomaly S1. On the Nova Scotia margin, northeast of SMART02 Line, the quasi-absence of SDRs northeast of SMART02 could be masked by the overlying salt or by other complexities (e.g., low signal-to-noise ratio or multiples) due to the thick sediments in the Scotian Basin. Therefore, some reduced volume of extrusives, as evidenced by the weakening ECMA anomaly in the northeast direction, might correspond to a thin layer of volcanic material as modelled by S. Delher (personal communication, 2010) but on this basis, we cannot dismiss the possibility of magmatic underplating, even if there is no clear thinned continental crust above. Figure 15 shows the presence of a thin layer of volcanics on top of the highly serpentinized mantle overlying the high velocity body.

From Holik et al. (1991) data on the Moroccan side, we have represented a 6.5-7 km thick oceanic crust, which is much thicker than the 4-km thick oceanic crust imaged on OETR2009 and SMART01 lines (Figure 12). Is the discrepancy in crustal thickness due to uncertainties in the processing of sonobuoy data of Holik et al. (1991) or to another reason as the lack of conjugacy for example?

From the same spreading center, it is impossible to create simultaneously a serpentinized mantle on the Nova Scotia side and an oceanic crust on the Moroccan side. The only possibility would be to first create the serpentinized mantle domain and then the oceanic domain. It is well known that there is

an asymmetry in the opening of the central Atlantic, in particular during the ECMA-BSMA (190-170 Ma) period. For many authors, the BSMA corresponds to an eastern ridge jump at ~ 170 Ma leaving crust from both ridge flanks between ECMA and BSMA (Vogt et al., 1971; Klitgord and Shouten, 1986; Roest et al., 1992; Schettino and Turco, 2009; Labails et al., 2010). For Labails et al. (2010), the initial opening phase between ECMA and BSMA is highly asymmetrical with in average 56% of the accretion taking place on the western side, but the asymmetry is variable from segment to segment. Because of the absence of serpentinized mantle on the Moroccan side and the presence of this asymmetry, we suggest that a major ridge jump occurred at the end of emplacement of the high velocity body at least from 31.5 to 34.5°N on the Moroccan side over a minimum distance of 300 km (Figures 8 and 11) where the oceanic crust has been inferred from Holik et al. data and on the conjugate NA side where the high velocity body has been identified (OETR2009 and SMART01 and 02 lines).

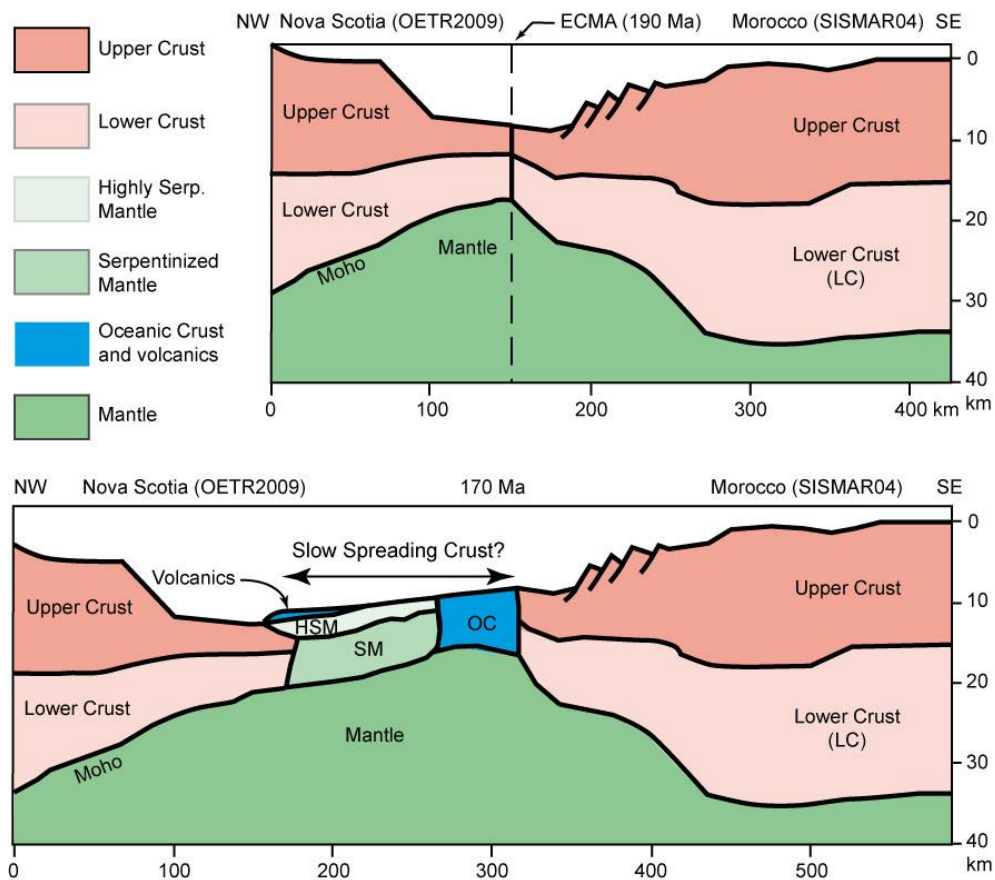


Figure 15: Crustal interpretation of conjugate velocity profiles SISMAR04 and OETR2009 at the time of emplacement of ECMA (190 Ma) and in early Middle Jurassic without syn- and postrift sediments. SM, serpentinized mantle; HSM, highly serpentinized mantle; OC, oceanic crust.

Figure 16 shows a schetch of the evolution of OETR2009-SISMAR04 conjugate margins. The rifting episode occurred between late Trias (Norian/Rhaetian limit, 203 Ma) and the formation of ECMA (Sinemurian/Pliensbachian limit, 190 Ma) (Figure 16a). During that period, salt deposited in a shallow water and restricted environment on both margins. Some volcanics belonging to the CAMP province intruded the salt layer and are contemporaneous of salt deposition. At the end of rifting, an eastward rift jump occurred in the north, where the lack of autochtonous salt was evidenced on the Nova Scotia

margin and where a restricted autochthonous salt province was identified between S1old and S1new (Figure 16b). Since 190 Ma, a transitional crust was emplaced in an slow spreading environment (1.4 cm/yr between ECMA and BSMA) (Figure 16c). It consists of asthenospheric mantle overlaid by highly serpentinized mantle resulting from the interaction of sea-water with peridotite. Some limited amount of melt was produced by decompression as shown by the ECMA magnetic modeling. There is no such serpentinized mantle on the Moroccan side, which means that at the end of the formation of the high velocity body, a second eastward rift jump occurred as attested by the ~45-km asymmetry observed on kinematic reconstructions (Labails et al., 2010). This ridge jump occurred along strike, over a distance of more than 300 km, i.e. the distance between OETR2009 and SMART02 lines, where a continuous high velocity body was identified (Figures 11 and 12). By using the kinematic parameters of rotation between ECMA and BSMA, the age of BSMA was established at 177 Ma (late Toarcian). Figure 16d shows that at the time of BSMA (170 Ma), already ~50 km of oceanic crust was emplaced. A consequence of this late eastward ridge jump is the absence of crust formed westward of S1 anomaly from 190 to 177 Ma. If this is true, the dipping reflectors observed in the oceanic crust (sometimes characterized as SDRs) and located east of the S1 anomaly are not related to the rifting episode but are linked to the emplacement of clearly post-rift oceanic crust.

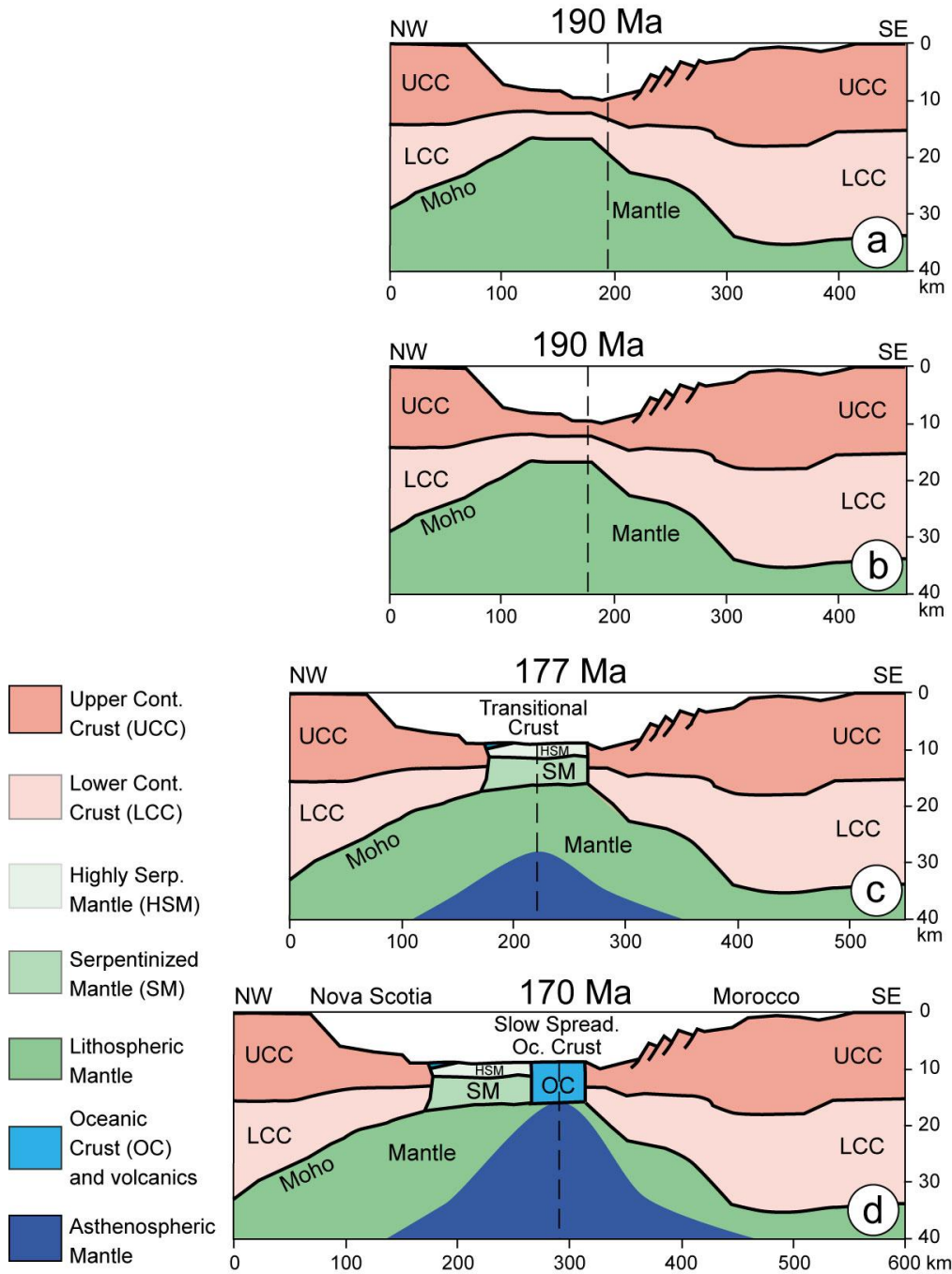
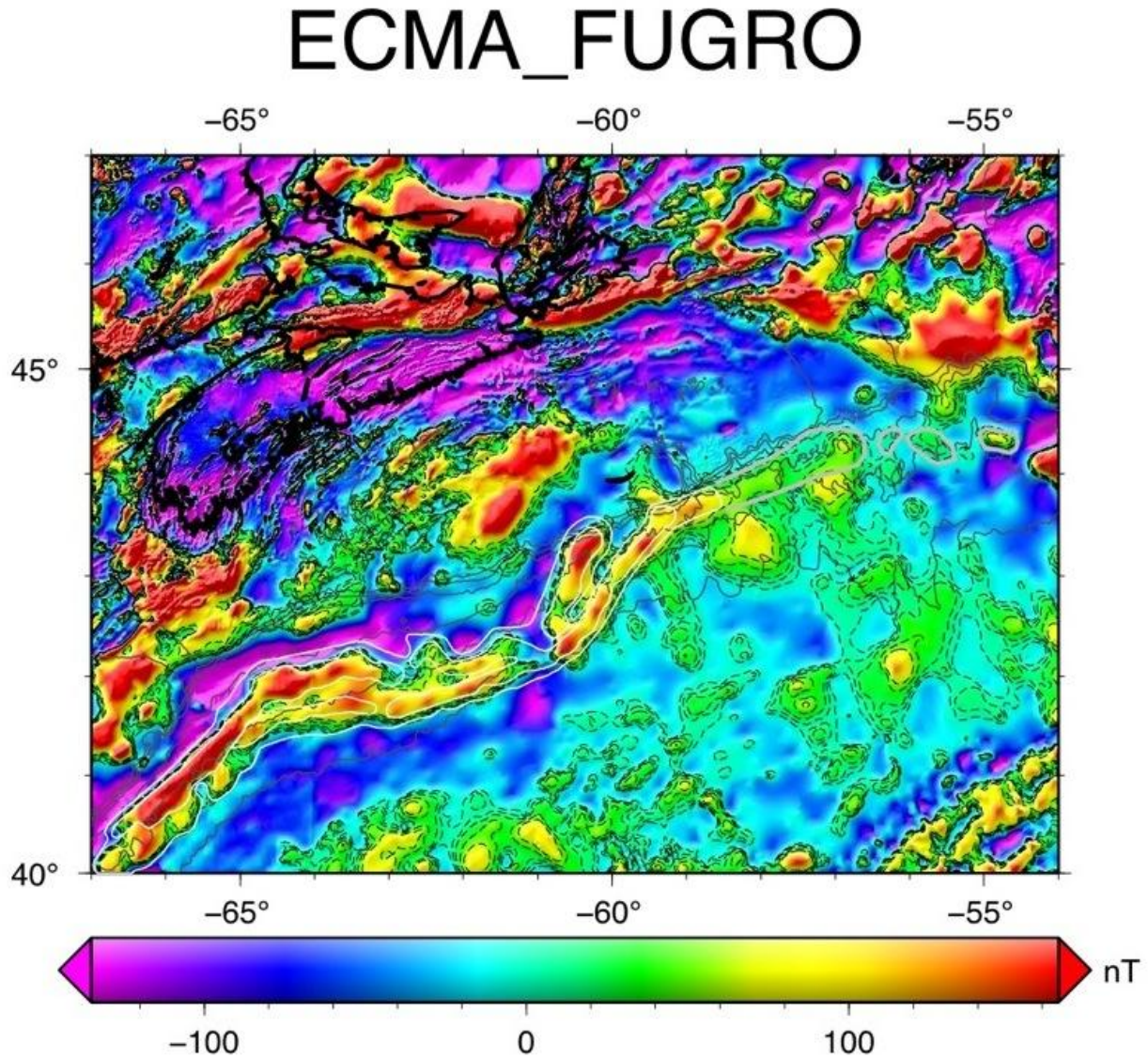


Figure 16: Scheme of formation and evolution of the Nova Scotia/Morocco conjugate margins. a) At the end of the rifting phase (chron ECMA, 190 Ma). b) after a ridge jump transferring part of the Nova Scotia thinned continental crust on the Moroccan side. c) At the end of emplacement of the lower crustal high velocity body (177 Ma, late Toarcian). d) After a ridge jump to the eastern side of the high velocity body and accretion of 50 km of typical oceanic crust (chron BSMA, 170 Ma, Bajocian).

2. Paleo-geographic reconstructions of the central and north Atlantic oceans

2.1. Northern prolongation of ECMA and WACMA

The magnetic grid of Verhoef et al. (1996) has been updated by introducing the detailed magnetic data acquired by Fugro in the northeastern prolongation of ECMA (Delher, 2010). A color-coded representation of this grid is shown in Figure 17 (an open color scale is used, see bottom of Figure 17). Thin continuous gray lines are bathymetric contours (200 m, 500 m and then every km, extracted from ETOPO1 data set (Amante and Eakins, 2009). In white is the portion of ECMA already identified by Sahabi et al. (2004) and in gray our interpretation of the northern ECMA prolongation. Dashed black lines are a selection of iso-values used to interpret the ECMA prolongation.



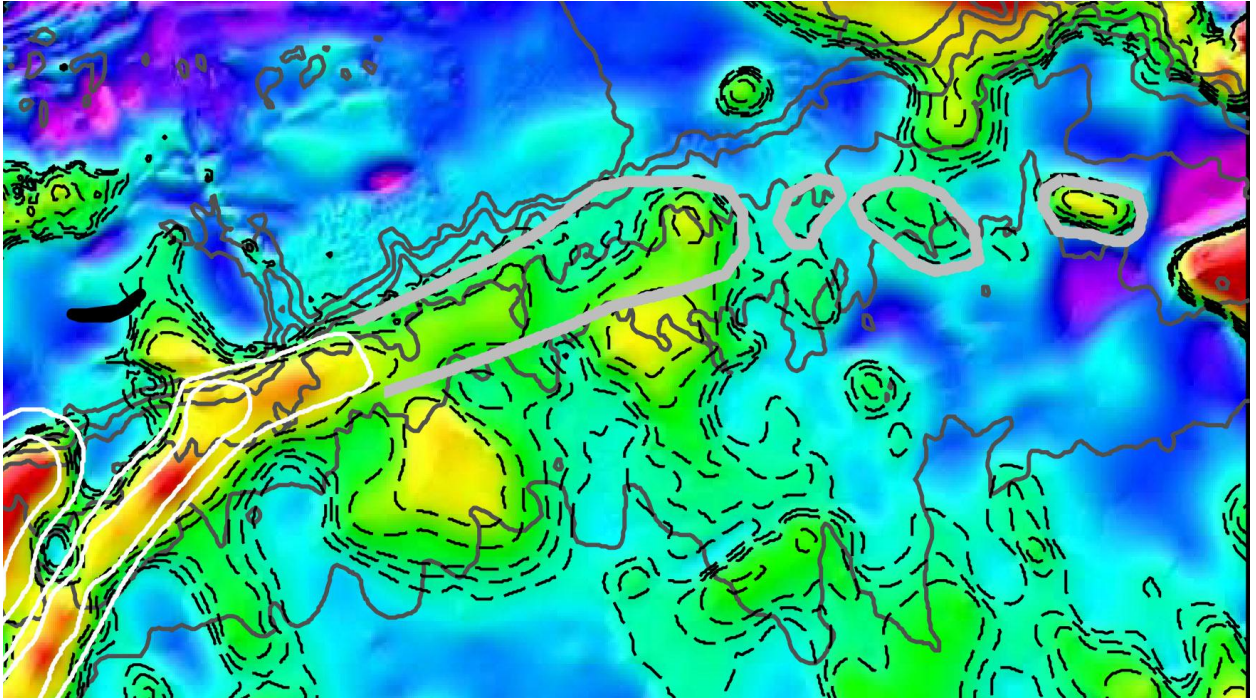


Figure 17: Updated magnetic grid of the northwestern central Atlantic ocean (Delher, 2010) (top) and detail of the northeastern termination of ECMA (bottom). Dashed lines are contoured magnetic anomalies and continuous black lines are bathymetric contours every km. In white the portion of ECMA already identified by Sahabi et al. (2004) and in gray what we suggest as a reasonable northern prolongation of ECMA.

For the purpose of comparison, Figure 18 shows the original Verhoef et al. (1996) magnetic data (1-minute grid), using the same display as in Figure 17. It clearly shows that the present interpretation benefits from the new data set and its higher resolution.

ECMA_Verhoef1m

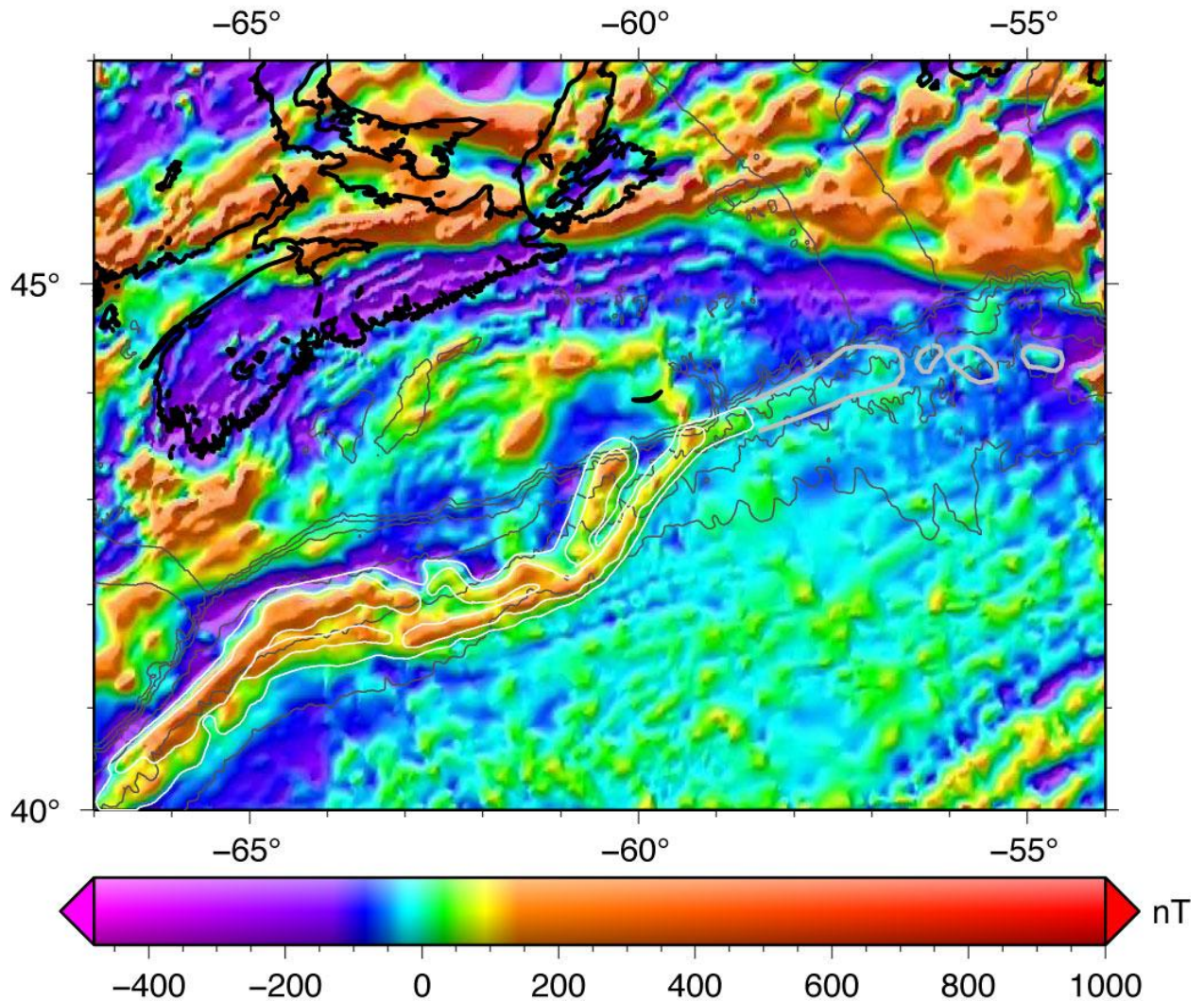


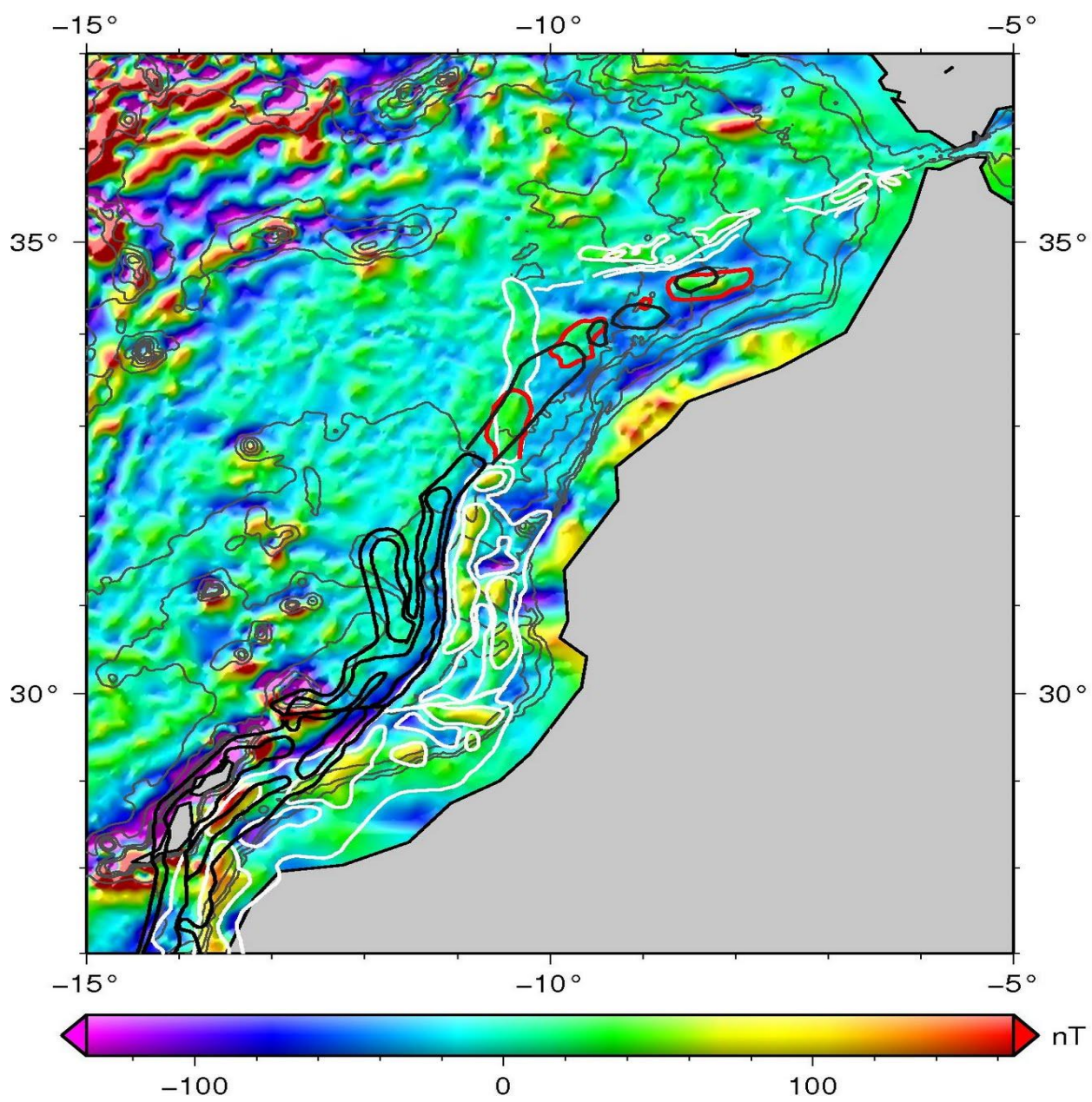
Figure 18: Magnetic anomaly map based on Verhoef et al. (1996) data. Same comments as in Figure 17.

East of 58.5°W (the eastern limit of Sahabi et al. (2004) ECMA identification), the amplitude of the ECMA is considerably reduced and associated magnetic anomalies broaden (Figure 17). Whereas the ECMA features a single positive anomaly that locally splits in two branches southward, the northward continuation we propose shows a rather different signature. First, the amplitude is two to three times lower than just southward. Second, the prolongation mostly appears as a linear borderline between a large negative anomaly to the north (blue in Figure 17) and a gently varying positive anomaly to the south (cyan in Figure 17). Thus, the northeastward prolongation of the ECMA is straightforward for its landward side and, using the magnetic iso-contours up to 56.5°W, could be define as a stripe not wider than the ECMA southward. Further east, only individualized, shorter extent, anomalies could be interpreted as a possible prolongation of the ECMA. Notice that the linear part of

the prolongation is parallel to the margin, whereas further east the prolongation slightly departs from the trend of the shelf break.

Thus, the nature of the ECMA is different east and west of 58.5°W. Refraction lines SMART01, SMART02 and OETR2000 are located west of 58°W. They show similar crustal features, in particular the presence of a high velocity body interpreted as serpentinized peridotite. S. Delher (2010, personal communication) suggested by forward modeling that the ECMA can be related to a very thin layer of volcanics located above the eastern part of the high velocity body, slightly extending to the northwest of the high velocity body. The ECMA may also be partly caused by the edge effect due to the juxtaposition of a magnetized serpentinized body and a poorly magnetized thinned continental crust. East of 58.5°W, the disconnected small magnetic anomalies interpreted as a possible prolongation of the ECMA suggest that both the high velocity body and the overlying volcanic layer are discontinuous.

Figure 19 shows the northeastern central Atlantic magnetic grid of Verhoef et al. (1996) updated with newly available data (courtesy of S. Delher, personal communication, 2010). We used the same color palette as in the preceding figures. The West African Coast Magnetic Anomaly (WACMA) is represented as a white line following the interpretation of Sahabi et al. (2004) and Labails et al. (2010) and as a red line for what we suggest to be the location of the WACMA in the north. The rotated ECMA is divided into two parts: one south of 30°N, is rotated as part of the AF plate with the NA/AF rotation parameters of Labails et al. (2010), while north of 30°N, the ECMA is rotated as part of the MES plate with the NA/MES rotation parameters of Labails et al. (2010). The two rotated portions of ECMA are drawn in black.



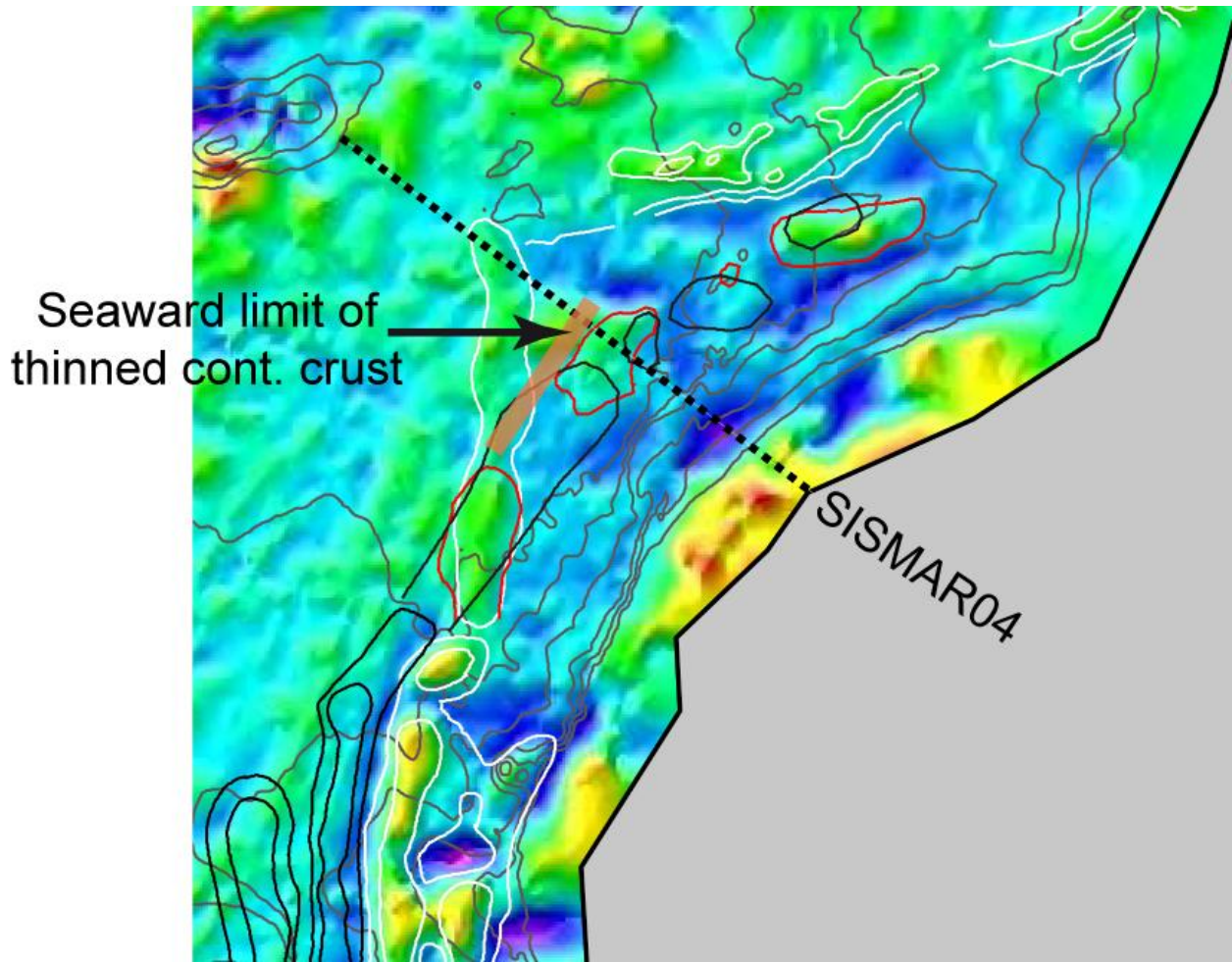


Figure 19: Northeastern central Atlantic magnetic anomaly map based on Verhoef (1996) data set updated by S. Delher (personal communication, 2010) (top) and detail of the northern portion of the WACMA (bottom). Same comments as in Figure 17. In gray, bathymetric contours every km. Continuous white lines are the WACMA contoured magnetic anomalies of Sahabi et al. (2004) and Labails et al. (2010) and continuous black lines are the rotated ECMA contoured magnetic anomalies (rotations parameters of Labails et al., 2010). In white the portion of ECMA already identified by Sahabi et al. (2004) and in red what we suggest as a possible northern prolongation of the WACMA. In brown, the seaward limit of the thinned continental crust based on the results of SISMAR04 refraction line and further southwest on the emergence of a crustal detachment fault on MCS SISMAR10 line.

North of 32.8°N , our WACMA identification (in red) does not follow Labails et al. (2010) interpretation but is parallel to the Moroccan continental slope. We follow the S anomaly of Roeser et al. (2002) up to 32.8°N . Roeser et al. (2002) do not identified S north of 33.4°N . As the northern portion of anomaly S of Labails et al. (2010) has not a counterpart on the NA side, we consequently question the conjugacy of the northern part of anomaly S and ECMA.

In the north, our proposed fit of ECMA and WACMA is much better than the one of Labails et al. (2010). However, it is not perfect as ECMA and WACMA are tangent in the south and overlapping to the north of 32.5°N . This discrepancy in the fit might be due to the different nature of ECMA (south and north of 32.5°N for the rotated ECMA) and/or to a wrong identification of the northern part of

WACMA. A better fit between ECMA and WACMA is hardly conceivable because we have to take into account the existence of a bend in both WACMA and rotated ECMA at 30.5°N latitude (cf. Figure 19), which prevents to move latitudinally the rotated ECMA with respect to WACMA. For these reasons, we suggest to keep Labails et al. (2010) parameters of rotation for chron ECMA both in the south (AF/NA) and in the north (MES/NA).

2.2. Reconstructions of the central and north Atlantic oceans

Before to establish the seven paleo-geographic maps mentioned in the deliverables we need to determine and/or to validate the rotation parameters of the five plates involved in this work, namely the Africa (AF), the Meseta (MES), the Iberia (IB), the Galicia Bank (GB) and the Flemish Cap (FC) plates with respect to the North America (NA) plate kept fixed in all the reconstructions. A large part of the work is already done for the AF/NA and MES/NA (Labails et al., 2010) but we need to establish the IB/NA, GB/NA and FC/NA parameters of rotation for times earlier than M0 because the oldest IB/NA parameters of rotations were properly established only from chron M0 onward (Srivastava et al., 2000). We have to test several hypotheses, in particular (i) What was the IB/MES motion during the Nova Scotia/Morocco rifting from late Triassic to early Jurassic ? (ii) Was Iberia attached to North America during most of the Jurassic, from Sinemurian (195 Ma) to around M25 (154 Ma) ? (iii) Was Iberia attached to Meseta and Africa from M25 or more recently to C13 (34 Ma, late Eocene) as demonstrated by Srivastava et al. (1990) ? (iv) What are the GB/IB parameters of rotation and the timing of motions ? (v) What are the FC/NA parameters of rotation and the timing of motions ?

2.2.1. Methodology used for plate reconstructions

Figure 20 shows the M0 reconstruction with the main kinematic elements (magnetic picks, fracture zones and bathymetric contours) used to calculate the parameters of rotations for specific chrons. Informations about the origin of the data and the making of the kinematic reconstruction maps are given in annex. We have adopted Labails et al. (2010) rotation parameters for the the MES/NA and AF/NA from the fit (Norian/Rhaetian limit, about 203 Ma) to chron M0. The IB/NA reconstructions are well constrained from M0 onward (e.g. Srivastava et al., 1988; Srivastava et al., 2000) but are badly constrained for older periods. The amplitude of magnetic anomalies belonging to the M sequence is considerably reduced on the IB side compared with the NA side, explaining the weak number of magnetic picks on the IB side. In addition, geophysicists were questioning both the seafloor spreading nature of these magnetic anomalies as well as their modeling with a seafloor spreading magnetic polarity reversal sequence until the acquisition of close to the sea-bottom magnetic profiles on the IB side (Whitmarsh et al., 1996; Russel and Whitmarsh, 2003) and the demonstration that these magnetic anomalies were due to the serpentinization process (formation of grains of magnetite) occurring at the time of mantle exhumation (Sibuet et al., 2007a). Even if the amplitude of magnetic anomalies is not the same than for typical seafloor spreading anomalies, Sibuet et al. (2007a) demonstrated that magnetic anomalies and lineations can be used to date the emplacement of exhumed mantle and consequently for kinematic reconstructions. Therefore, we propose to revise the IB/NA kinematic story for periods older than chron M0.

M0 reconstruction

Parameters of rotation of Srivastava et al. (2000) for IB/NA, Srivastava et al. (1992) for EU/NA are used for the M0 reconstruction (Figure 20). GB and FC are in their present-day positions with respect to IB and NA respectively.

M11 and M22 reconstructions

Reasonable hypotheses have to be assumed for the M21-M0 period where magnetic picks exist between IB and NA:

- Due to the lack of fracture zones pattern between IB and NA and to the extremely weak number of magnetic picks on the IB side, mostly identified on deep-tow magnetic data, it is impossible to unambiguously fit conjugate magnetic lineations or picks. However, by comparing the distribution of picks on both sides, the degree of asymmetry is weak. Thus, we have assumed a symmetrical seafloor spreading, even if we know that it is not true for MES/NA for example.
- M22 has been extrapolated from M0 to M21 picks. Fits at M11 and M22 have been computed with respect to the M0 fit by doubling the M0-M11 and M0-M22 distances of the NA side and, in the absence of fracture zones, by assuming that motions were parallel to the Newfoundland-Gibraltar FZ. The final results appear in Figure 21, showing a lateral continuity between northern Iberia and northeastern Flemish Cap bathymetric trends, supporting the hypothesis of IB/NA motions occurring parallel to the the Newfoundland-Gibraltar FZ.
- GB/IB closure by assuming 105 km of extension between GB and IB during the M11-M22 period (Murillas et al., 1990, Sibuet et al., 2007b) and a pole of rotation at 90° as the width of the N-S trending Interior Basin (located between IB and GB) is constant from north to south. Thus, at chron M11, GB is in its present-day position with respect to IB and at chron M22 in its full closure position.
- the FC/NA angle of rotation has been adjusted to fit the 3000-m isobaths west of GB and southeast of FC.

Reconstruction at closure (203 Ma)

The fit at closure (203 Ma) have been computed by assuming:

- fit of the NA and IB 3000-m isobaths and a lateral continuity between the northern Iberia and northeastern Flemish Cap bathymetric trends.
- FC/NA closure as established by Sibuet et al. (2007b)
- GB/IB closure as established above.

The results displayed in Figures 22 and 23 are particularly satisfactory, with an excellent fit of the 3000-m isobaths of southeastern Flemish Cap and west Galicia Bank and of IB and NA.

ECMA reconstruction

Salt deposits not only occurred on the Nova Scotia and Morocco margins from Rhaetian to Sinemurian but also between IB and NA during the same period (Tucholke and Whitmarsh, 2011), suggesting rifting also occurred between IB and NA from 203 Ma to chron ECMA. Without any further constraint, we have assumed that IB and MES were moving together during this period, i.e. that we have a continuity in amount and direction of extension along the whole NA margin from Nova Scotia to Grand Banks. The FC/NA rotation angle is adapted in order to keep the closure between FC and GB.

BSMA reconstruction

Locations of IB/NA at chrons ECMA and M22 are so close that the resulting 20 km of differential motion, almost parallel to the Newfoundland-Gibraltar FZ, can be distributed at any time between chrons ECMA and M22, possibly just before M22. In this hypothesis, IB, which was attached to MES prior chron ECMA, became quasi attached to NA from chron ECMA to chron M22. Closure of GB/IB is complete and the FC/NA rotation angle is adapted to keep the closure between FC and GB.

C34 reconstruction

Parameters of rotation of Klitgord and Shouten (1986) for AF/NA, Srivastava et al. (1990) for IB/NA and Srivastava et al. (1988) for EU/NA are used for the C34 reconstruction. MES/NA have been computed in order to keep the same MES/AF position than for chron M0. GB and FC are in their present-day positions with respect to IB and NA respectively.

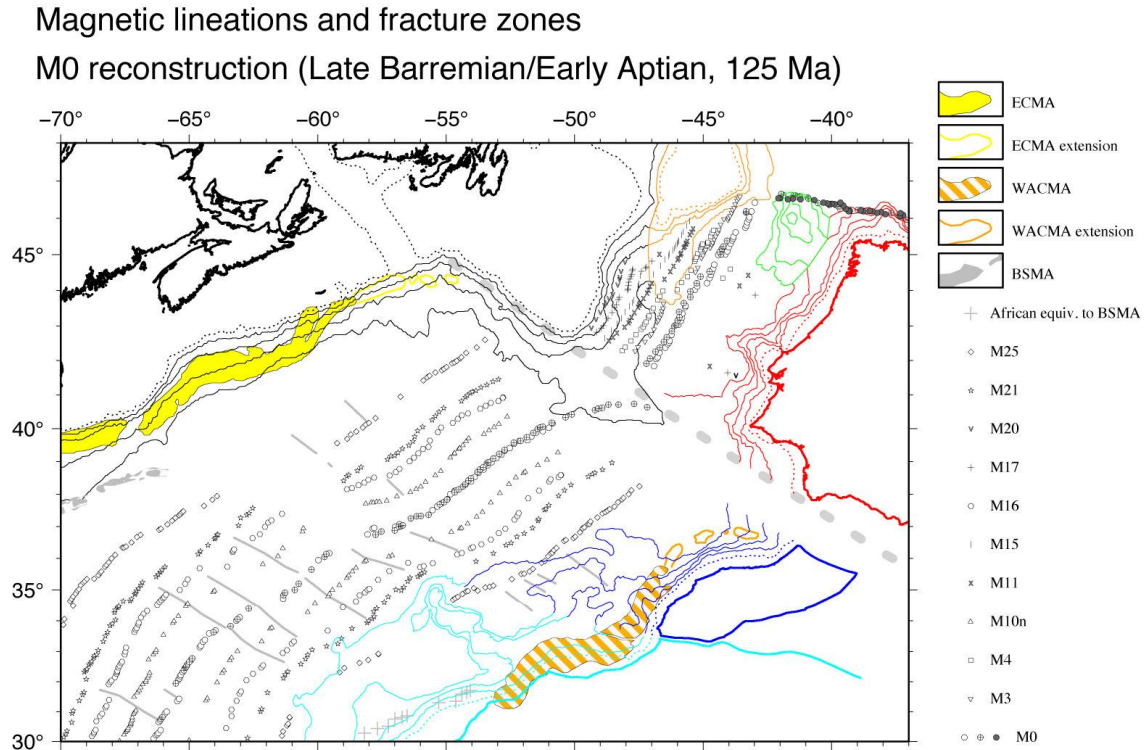


Figure 20: Reconstruction of the central and north Atlantic oceans at chron M0 (118 Ma). The north American plate is fixed. Africa, Meseta, Iberia, Galicia Bank and Flemish Cap are respectively in cyan, blue, red, green and orange. Dotted lines for isobath 200 m and dashed lines for isobaths 1000 to 4000 m. The thick dotted gray line is the Nova-Scotia/Gibraltar fracture zone, while the thin gray lines are minor fracture zones. Magnetic anomaly identifications are displayed on the right-hand side of the figure.

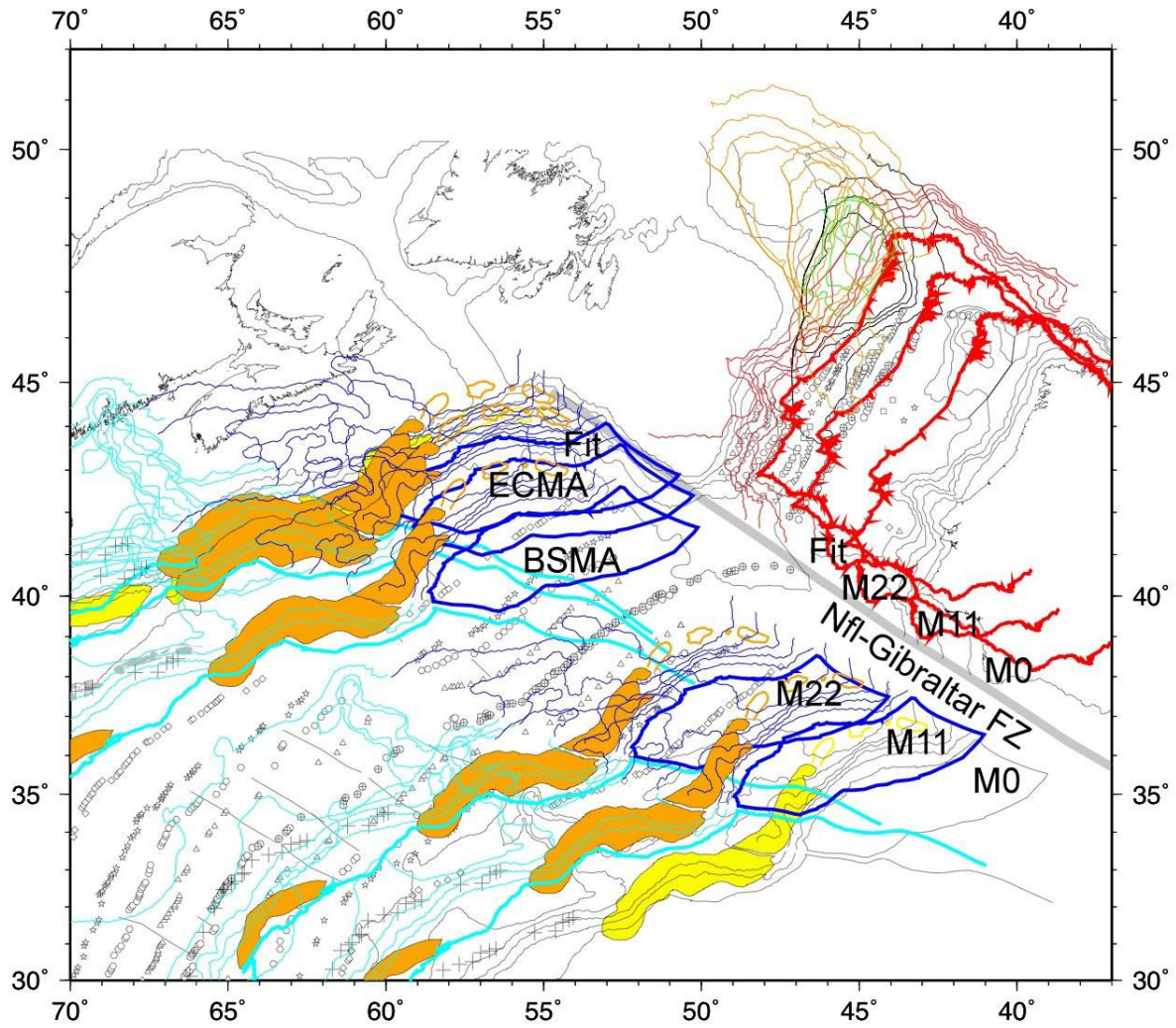


Figure 21: Summary of MES, AF and IB positions with respect to Eurasia for periods spanning from the fit of the central Atlantic to M0. Same legend and symbols than in Figure 20.

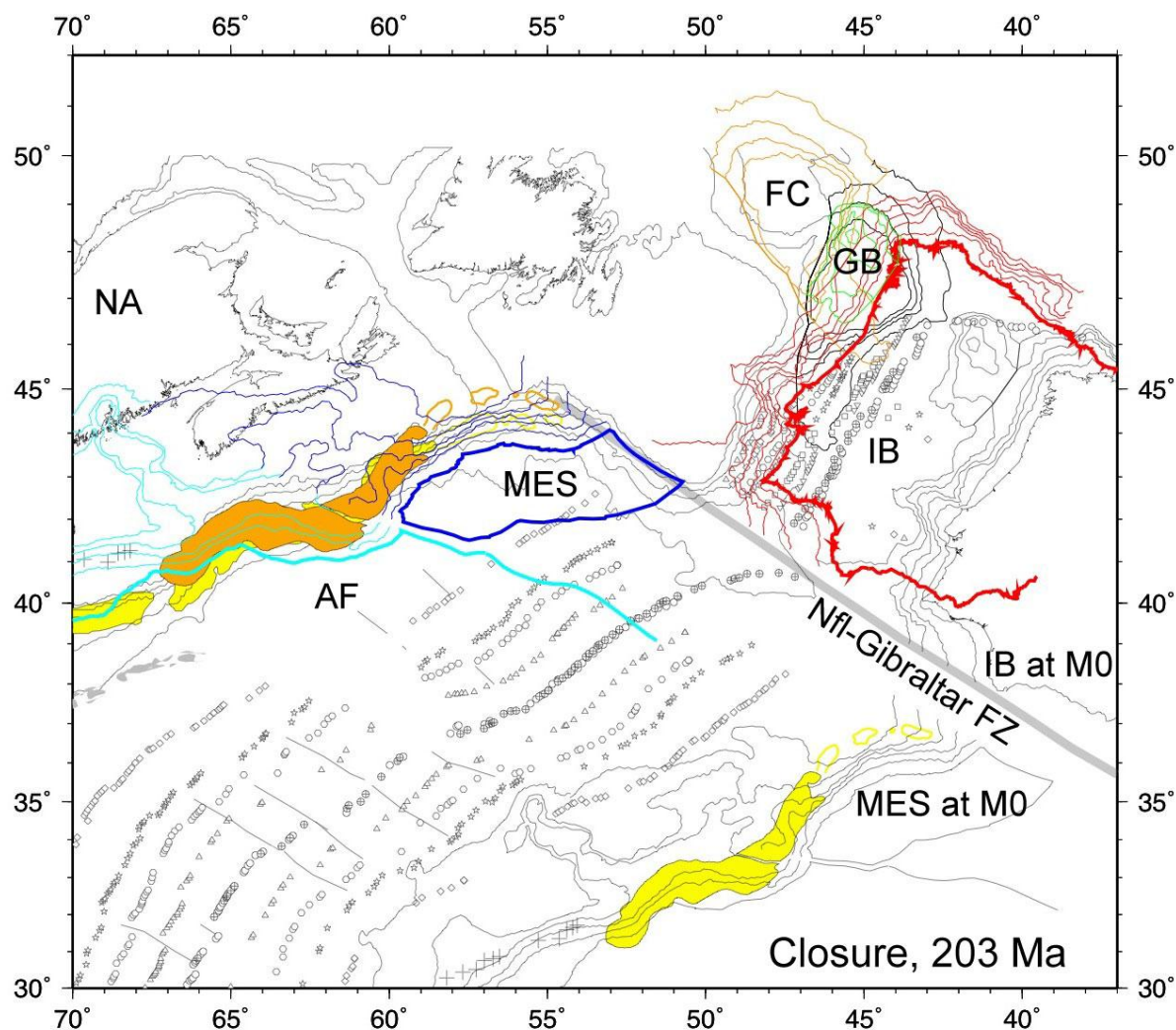


Figure 22: Kinematic reconstruction at closure (Norian/Rhaetian limit, about 203 Ma) superposed on the M0 reconstruction. Same legend and symbols than in Figure 20.

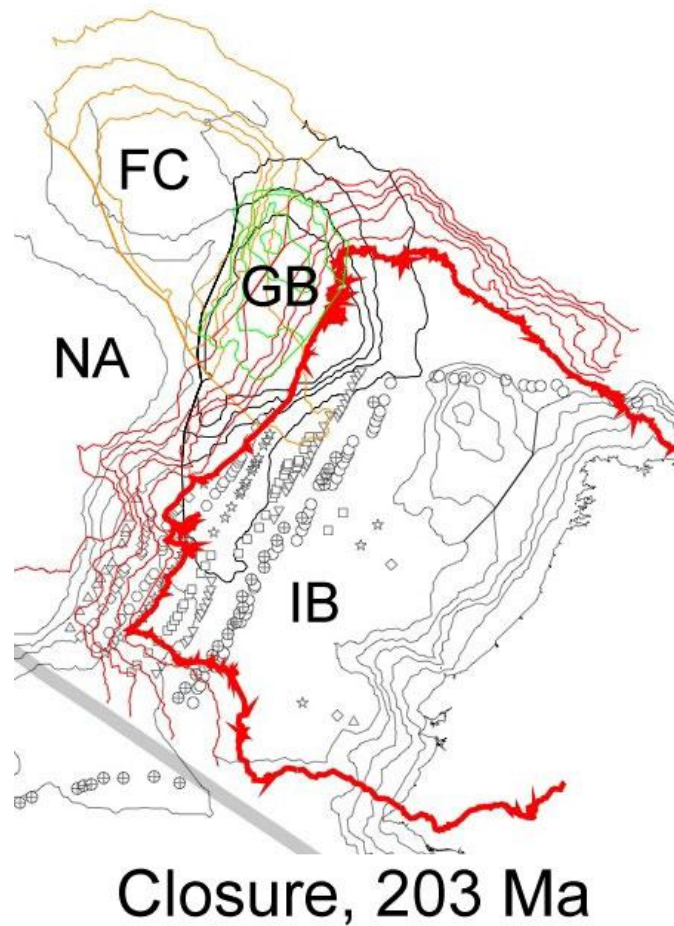


Figure 23: Detail of the kinematic reconstruction between IB and NA at closure (Norian/Rhaetian limit, about 203 Ma). Note the quality of the fit of isobaths between the four NA, IB, GB and FC plates. Same legend and symbols than in Figure 20.

2.3. Paleo-geography of salt deposits at chrons ECMA and BSMA

Figures 24, 25 and 26 show the distribution of salt deposits published in the public literature between MES-AF and Nova Scotia margins and between IB and NA on kinematic reconstructions at chrons ECMA and BSMA, respectively. The late Triassic-early Jurassic salt was deposited during the rifting episode of the surrounding margins of Nova Scotia, Morocco and Iberia but also in the Grand Banks, Morocco, Algarve, Lusitanian and Porto intra-continental basins. Detailed origin of the data is given in annex.

Figure 26 shows the detail of the BSMA salt reconstruction. The dark red polygon on the Moroccan side corresponds to the area where the autochthonous salt is located seaward of the limit of the Moroccan thinned continental crust as displayed in Figure 1. This dark red polygon has been arbitrarily translated on the Nova Scotia margin, where there is an indentation in the autochthonous salt boundary of Albertz et al. (2010) corresponding to a lack of autochthonous salt. The translated dark red polygon fits well with the area without autochthonous salt. On seismic profiles shot perpendicularly to the margin and across the area with a lack of autochthonous salt, ~50 km of thinned continental crust and associated overlying salt are missing with respect to what is observed on seismic profiles shot outside this area.

This distance corresponds to the width of the dark red polygon, suggesting that a ~50 km ridge jump may have occurred in this area at the end of chron ECMA, before mantle exhumation and formation of volcanics by decompression melting (Figure 27). If these observations are correct, the fit at chron ECMA must be slightly changed in the future, with a position of MES/NA moved ~100 km to the southwest.

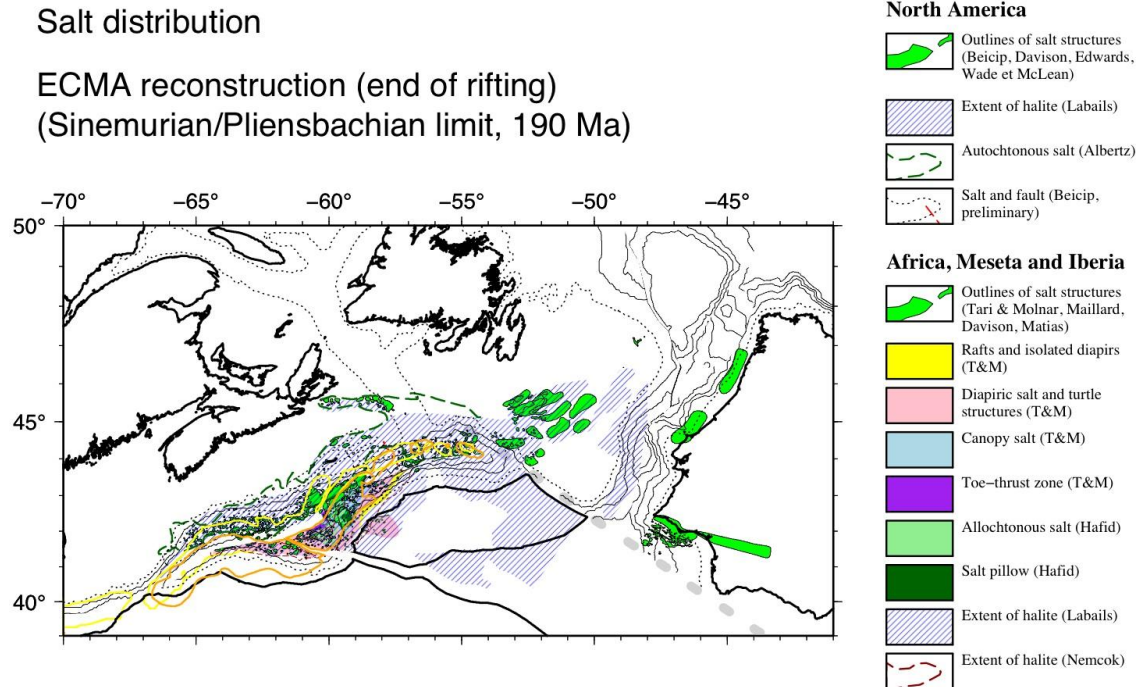


Figure 24: Distribution of salt deposits at the end of their deposition (chron ECMA, 190 Ma, Sinemurian/Pliensbachian limit). On the Grand Banks, south of the Cumberland ridge, which limits the Orphan Basin to the South, some salt deposits are not shown because the information is not released by the oil industry.

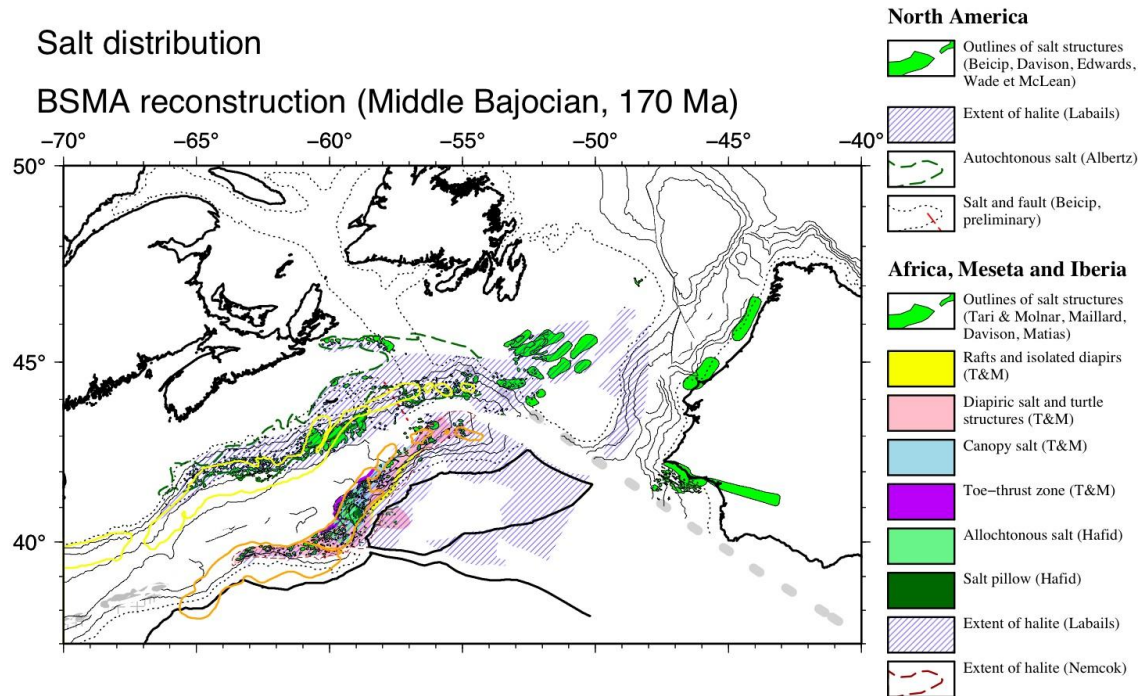


Figure 25: Distribution of salt deposits on the BSMA reconstruction (170 Ma, Middle Bajocian), about 20 Ma after the end of salt deposition.

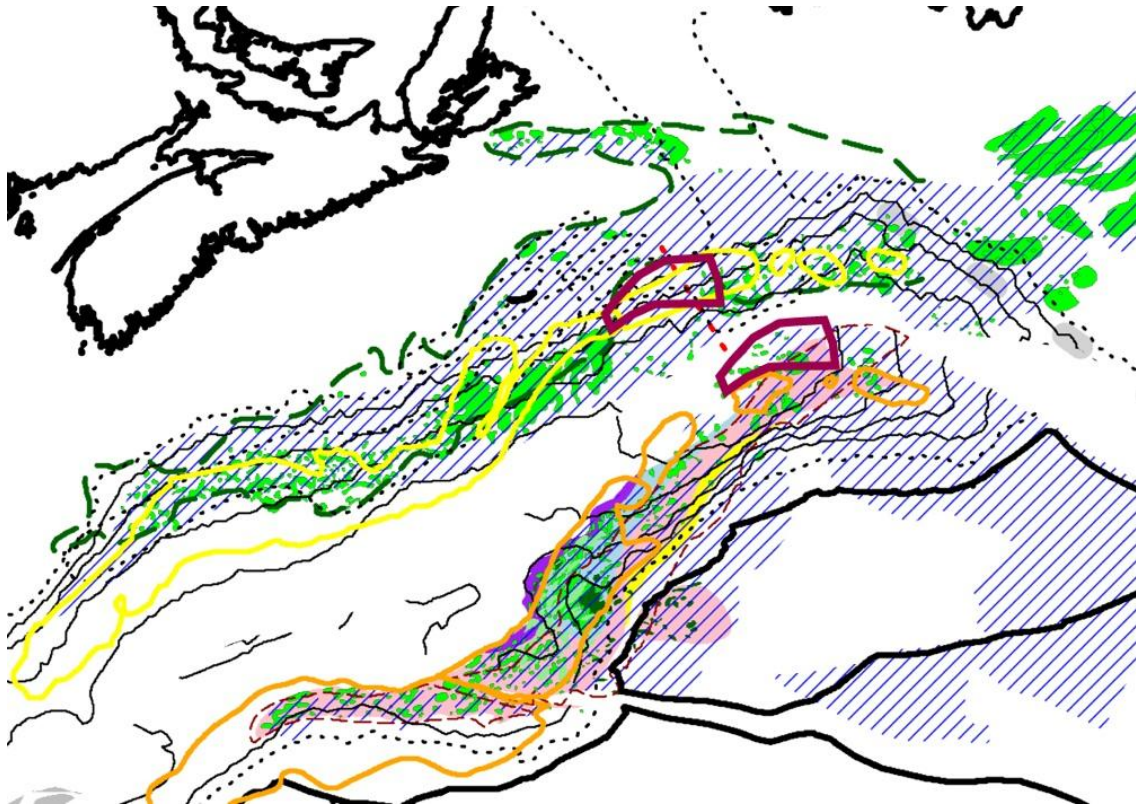


Figure 26: Detail of the distribution of salt deposits on the BSMA reconstruction (170 Ma, Middle Bajocian). The dark red polygon on the Moroccan side corresponds to the area where the autochthonous salt is located seaward of the thinned Moroccan continental crust and which might have been emplaced

after a ridge jump occurring at chron ECMA. The dark red polygon translated on the NA side fits well with the area without autochthonous salt.

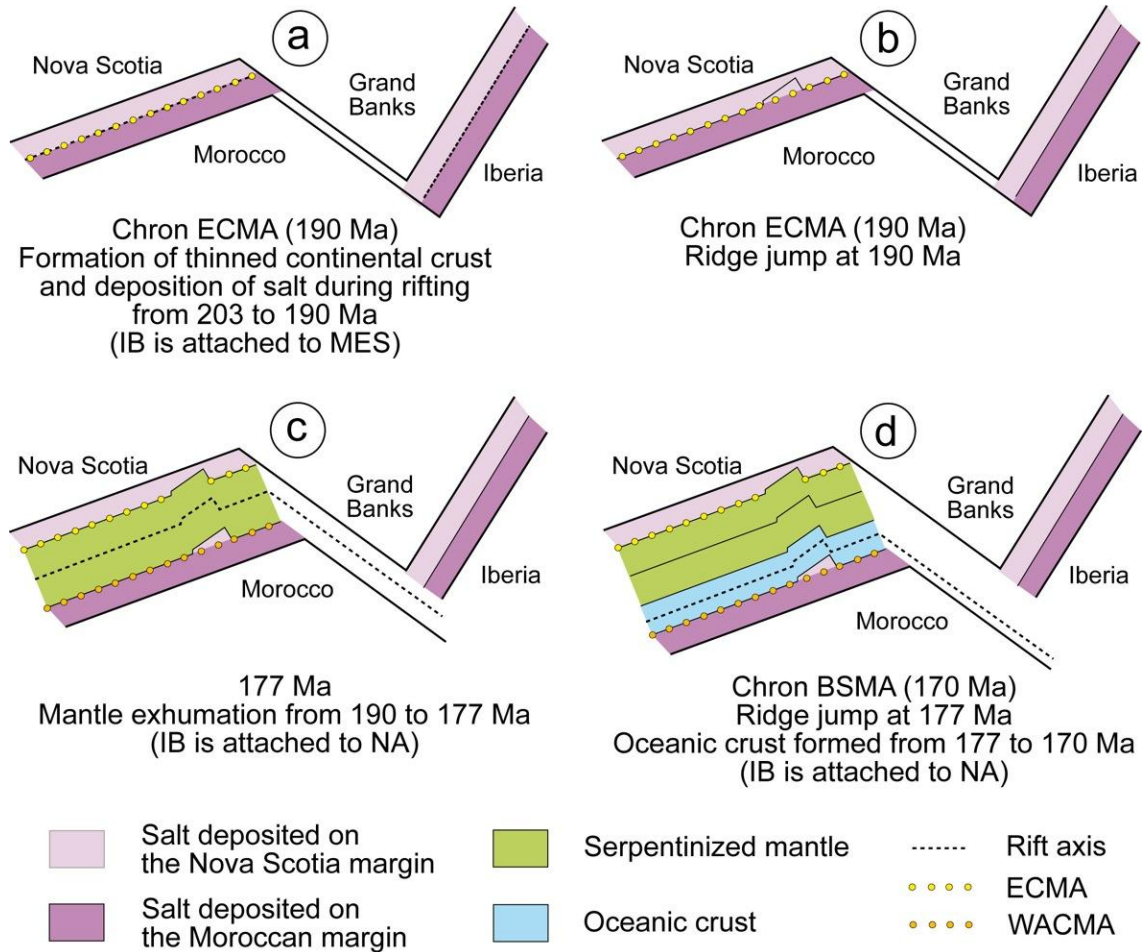


Figure 27: Sketch showing the two eastward ridge jumps at 170 and 177 Ma, explaining the presence of salt features westward of the Moroccan thinned continental crust boundary and the absence of serpentinized peridotite on the Moroccan side, respectively.

2.4. Kinematic and magnetic maps

Figures 28 to 33 show the resulting kinematic reconstructions from chrons ECMA to C34. Figures 34 to 40 show the magnetic reconstructions from the fit (203 Ma) to chron C34.

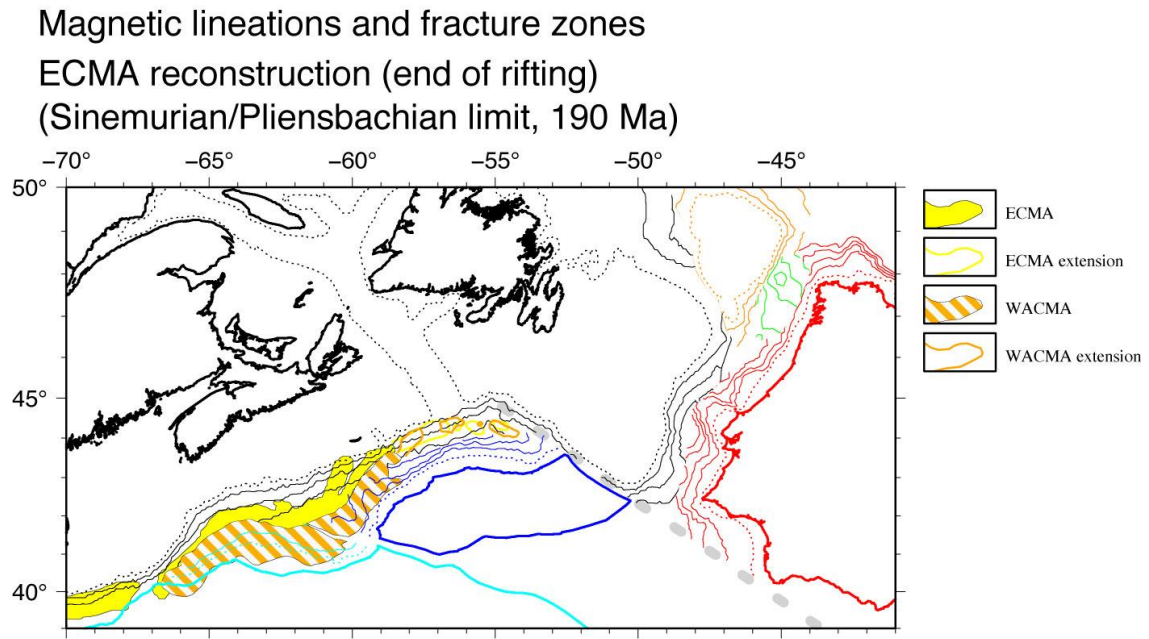


Figure 28: Kinematic reconstruction at chron ECMA (Sinemurian/Pliensbachian limit, 190 Ma).

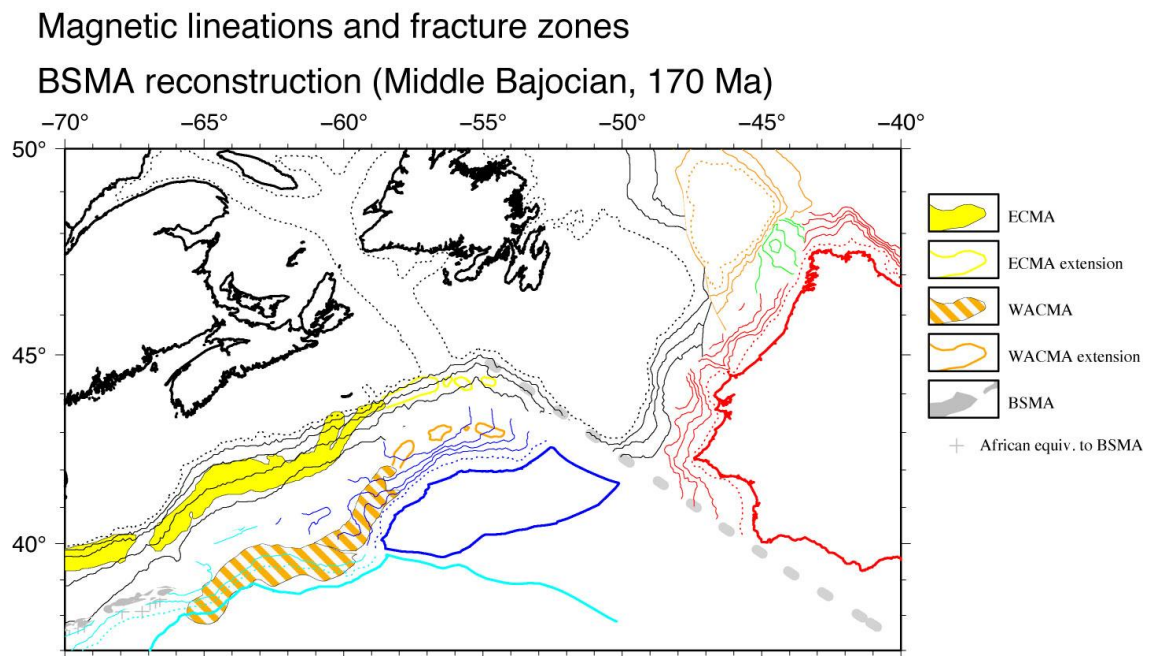


Figure 29: Kinematic reconstruction at chron ECMA (Sinemurian/Pliensbachian limit, 190 Ma).

Magnetic lineations and fracture zones
M22 reconstruction (Tithonian, 150 Ma)

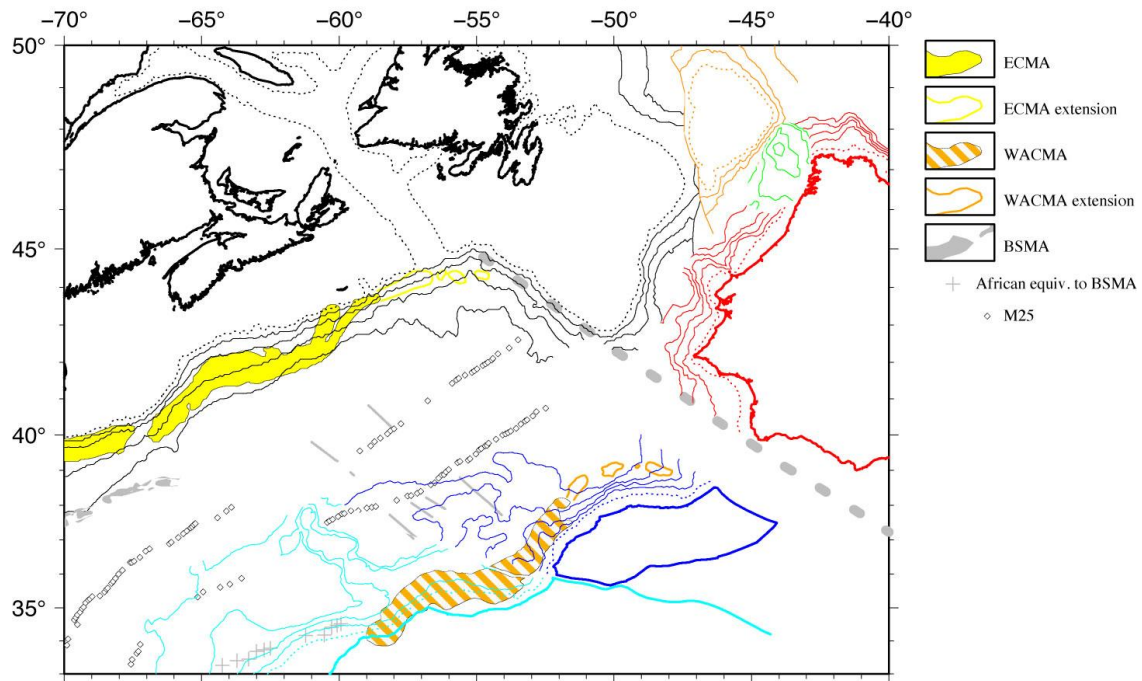


Figure 30: Kinematic reconstruction at chron BSMA (middle Bajocian, 170 Ma).

Magnetic lineations and fracture zones
M11 reconstruction (Valanginian, 136 Ma)

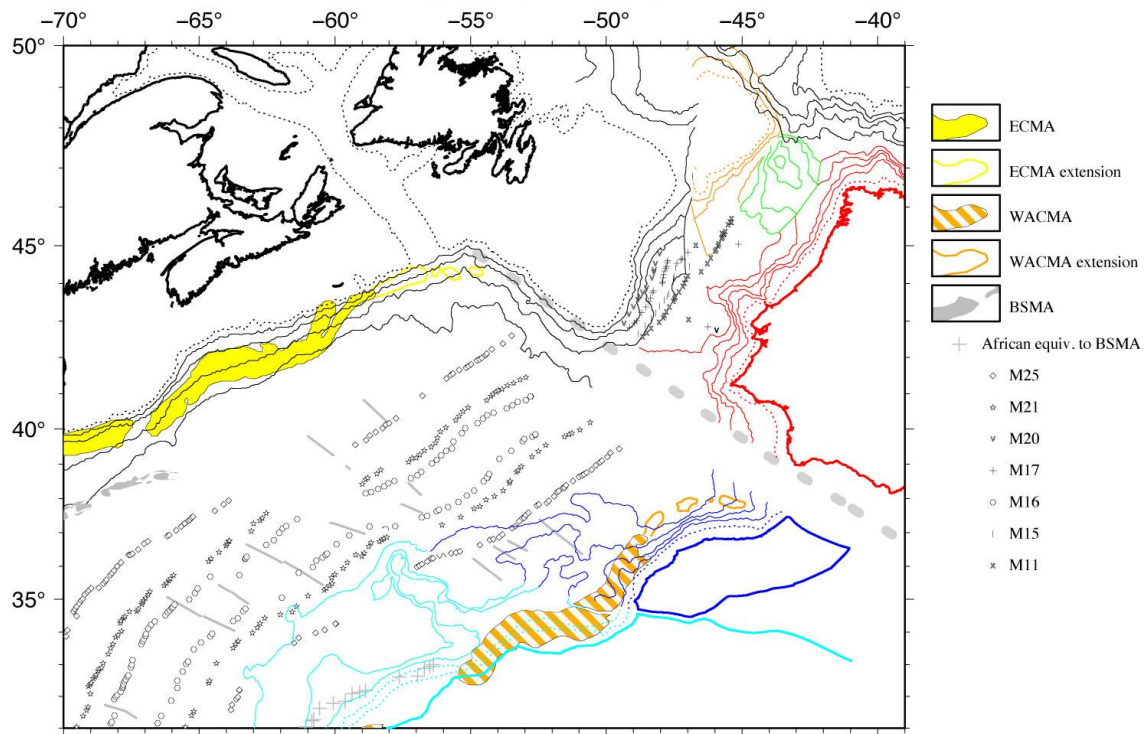


Figure 31: Kinematic reconstruction at chron M11 (middle Valanginian, 136 Ma).

Magnetic lineations and fracture zones

M0 reconstruction (Late Barremian/Early Aptian, 125 Ma)

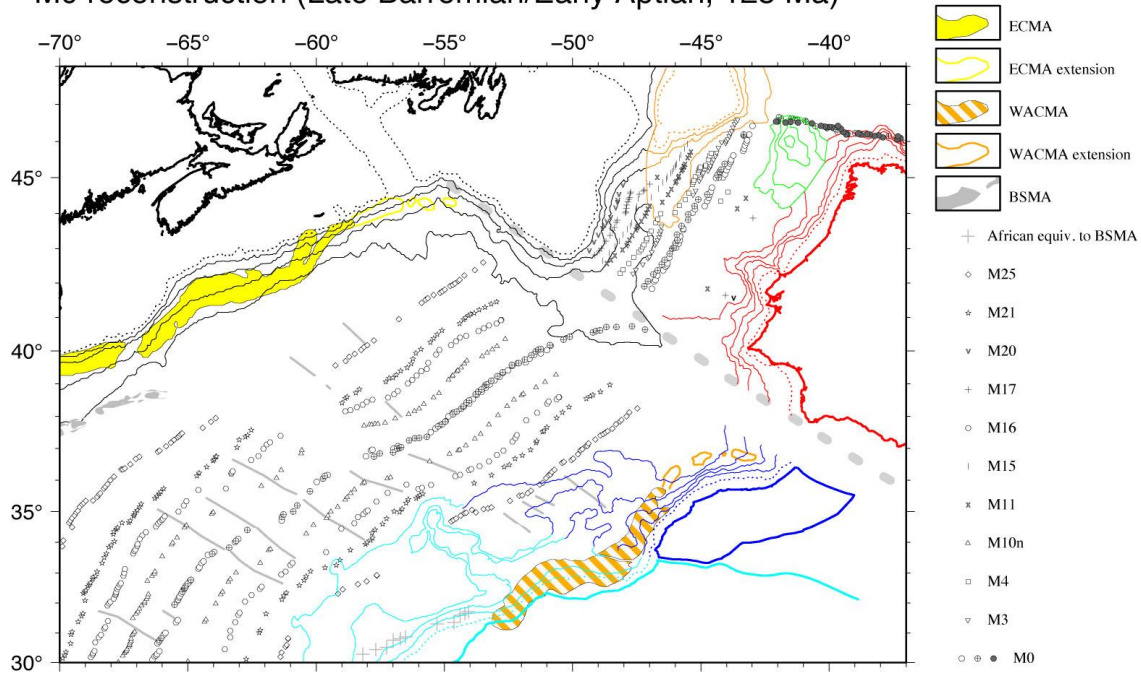


Figure 32: Kinematic reconstruction at chron M0 (late Barremian/early Aptian, 125 Ma).

Magnetic lineations and fracture zones

C34 reconstruction (Santonian, 83.5 Ma)

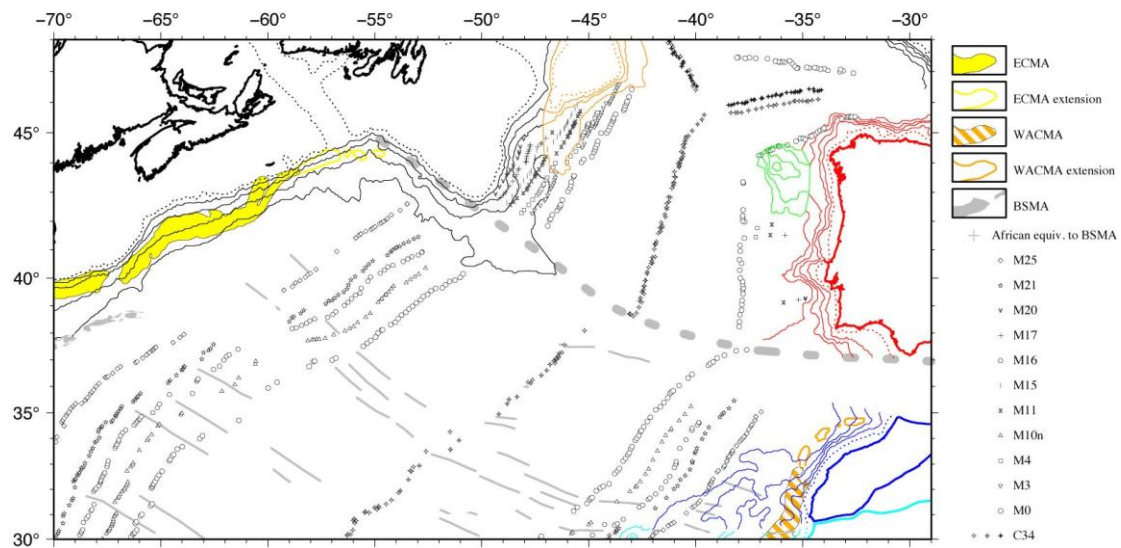


Figure 33: Kinematic reconstruction at chron C34 (Santonian, 83.5 Ma).

Magnetic anomalies

Pre-rift configuration: Late Triassic
(Norian/Rhaetian limit, about 203 Ma)

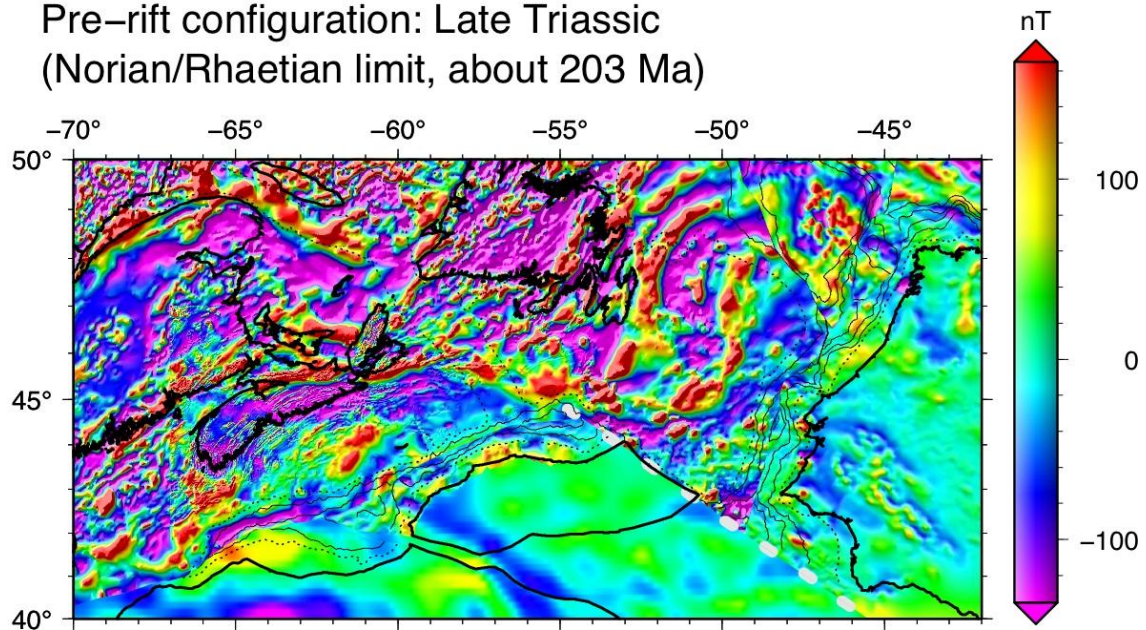


Figure 34: Magnetic anomaly map on kinematic reconstruction at the Norian/Rhaetian limit (203 Ma).

Magnetic anomalies

ECMA reconstruction (end of rifting)
(Sinemurian/Pliensbachian limit, 190 Ma)

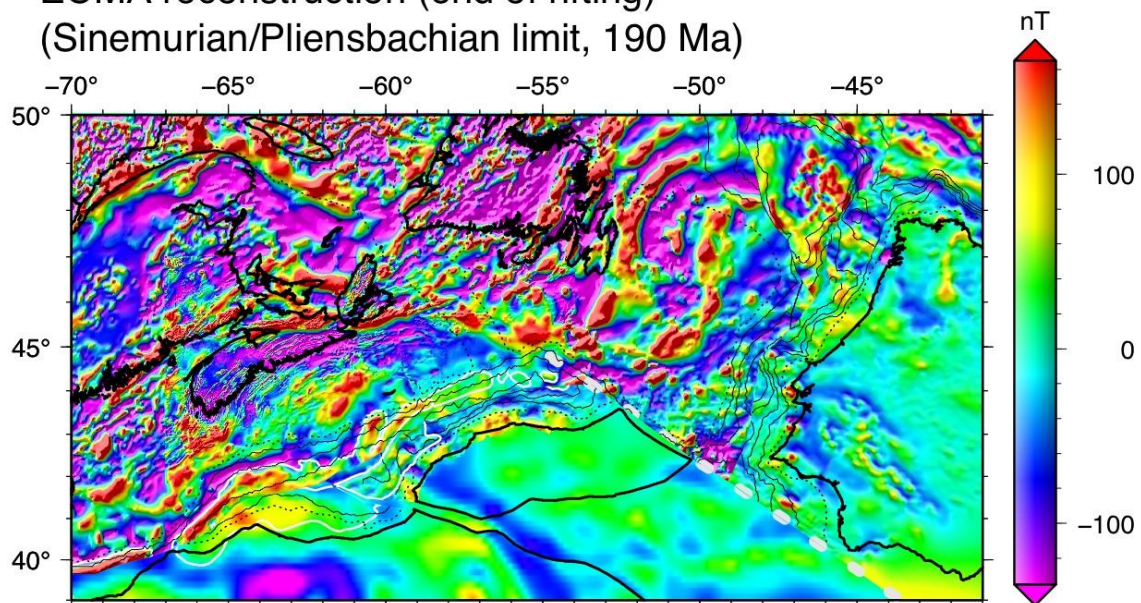


Figure 35: Magnetic anomaly map on kinematic reconstruction at chron ECMA (Sinemurian/Pliensbachian limit, 190 Ma).

Magnetic anomalies

BSMA reconstruction (Middle Bajocian, 170 Ma)

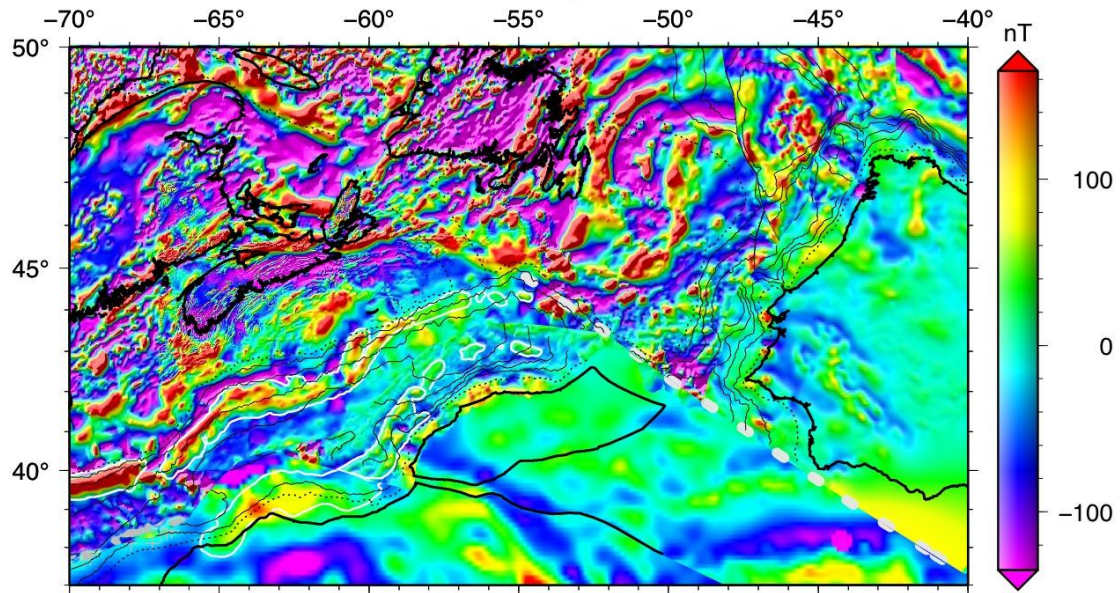


Figure 36: Magnetic anomaly map on kinematic reconstruction at chron BSMA (middle Bajocian, 170 Ma).

Magnetic anomalies

M22 reconstruction (Tithonian, 150 Ma)

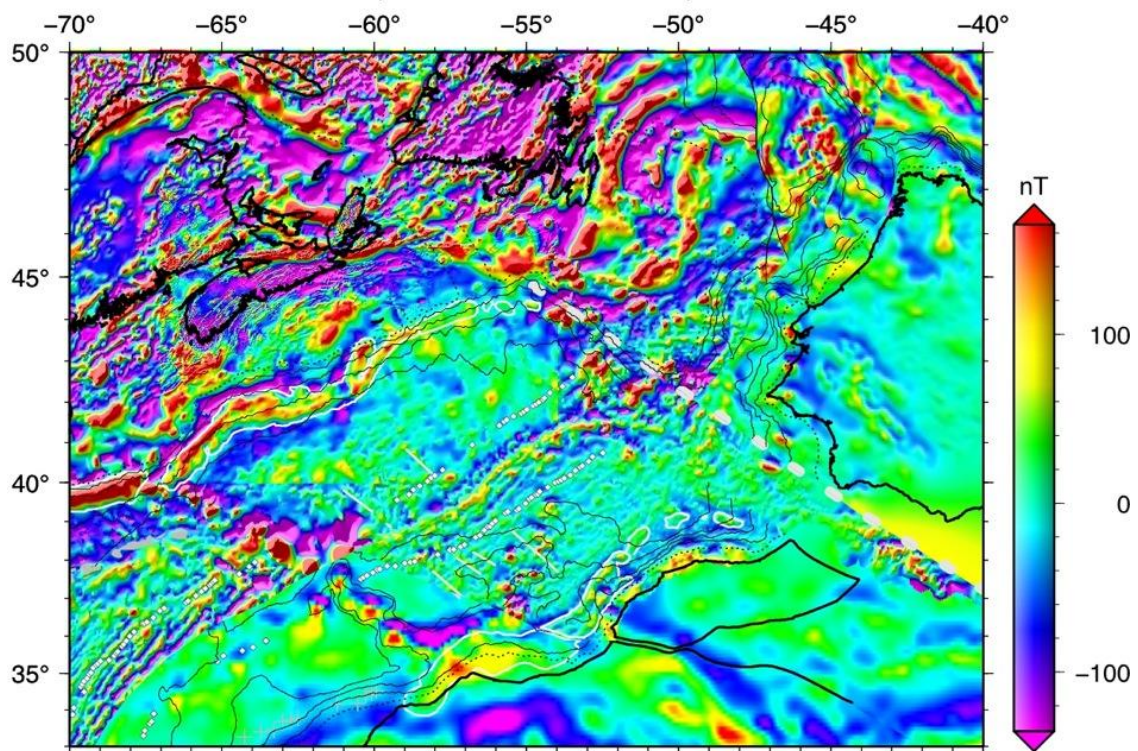


Figure 37: Magnetic anomaly map on kinematic reconstruction at chron M22 (middle Tithonian, 150 Ma).

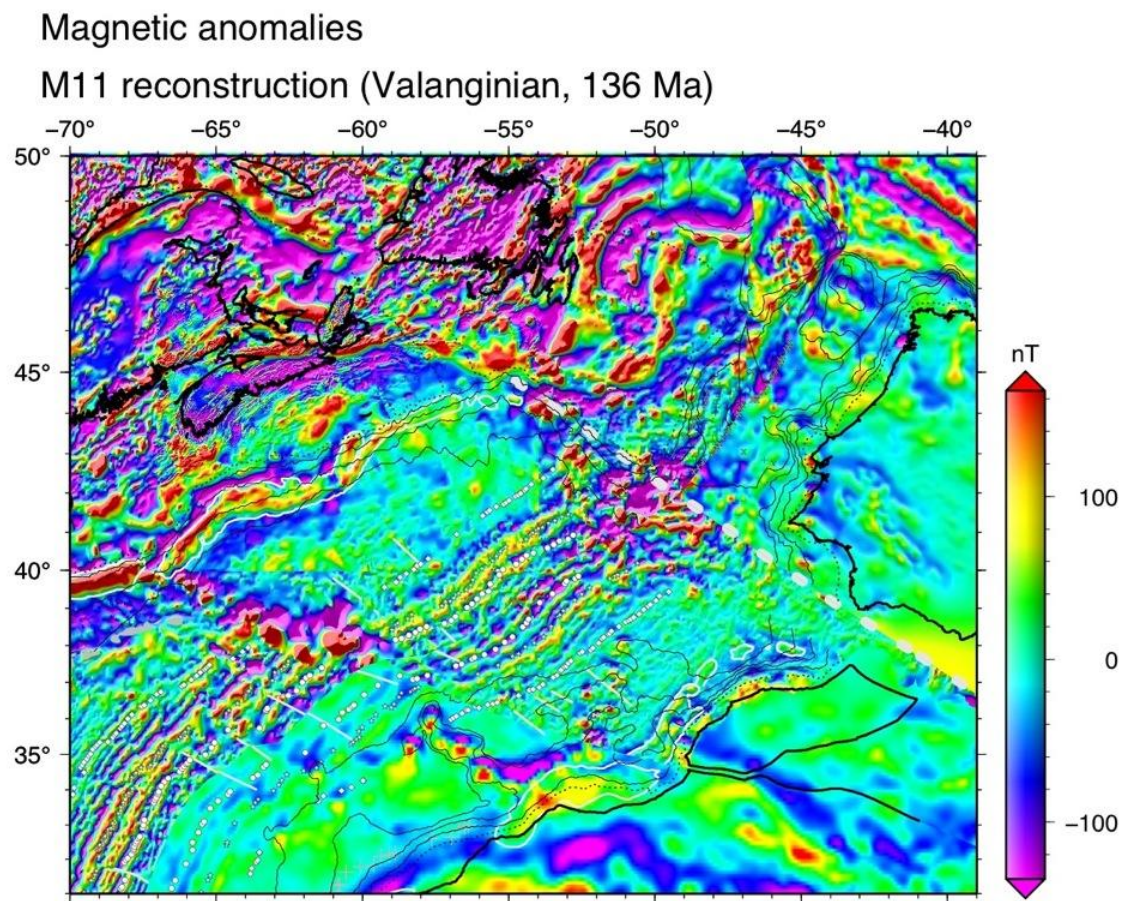


Figure 38: Magnetic anomaly map on kinematic reconstruction at chron M11 (Valanginian, 136 Ma).

Magnetic anomalies

M0 reconstruction (Late Barremian/Early Aptian, 125 Ma)

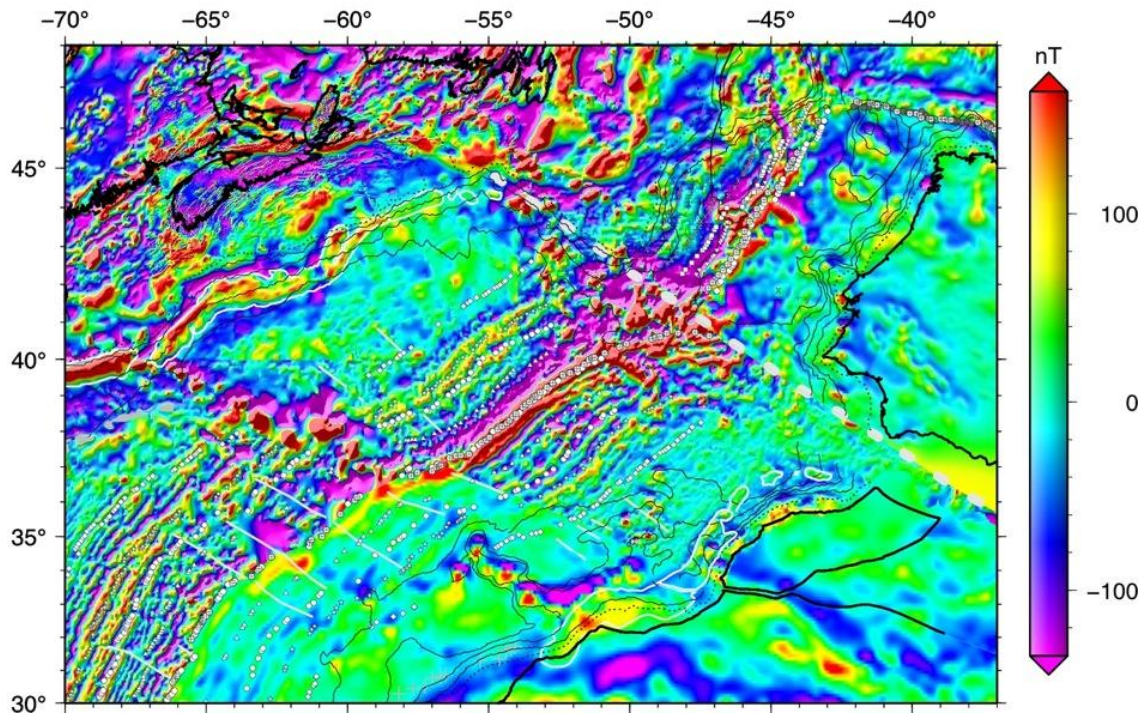


Figure 39: Magnetic anomaly map on kinematic reconstruction at chron M0 (late Barremian/early Aptian, 125 Ma).

Magnetic anomalies

C34 reconstruction (Santonian, 83.5 Ma)

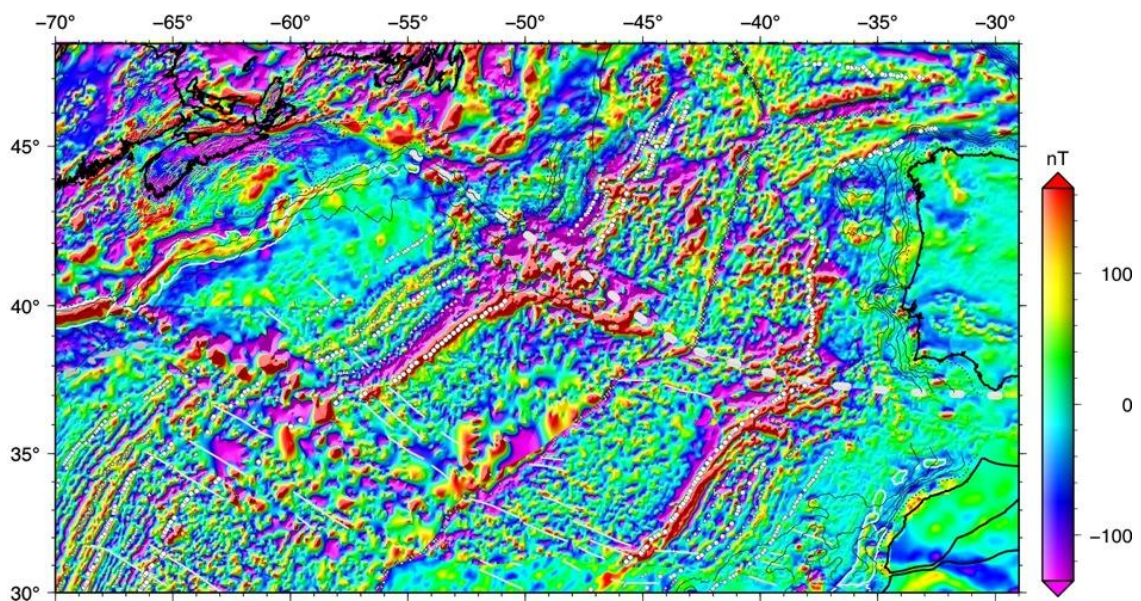


Figure 40: Magnetic anomaly map on kinematic reconstruction at chron C34 (Santonian, 83.5 Ma).

2.5. Paleo-geographic maps

The paleo-geographic maps presented in Figures 41 to 47 are basically constructed from Gradstein et al. (1990) maps. The main difference between the two sets of maps is the more accurate kinematics used in our set of maps from Late Triassic to chron M0 (see Annex B). For each map, we will not repeat the paleo-facies detailed descriptions, which appear in Gradstein et al. (1990) and to which the reader is conveyed.

Figure 41 shows the plates configuration before any extension. The bathymetric contours give the shape of the present-day edges of continents, not the true depth, which was close to zero at that time, with the presence of epi-continental seas of a few meters to a few tens of meters deep. One of the main point coming out from our paleo-geographic maps is that, during the rifting period (late Triassic to the Sinemurian/Pliensbachian limit, Figure 42), an elongated depression was created between Morocco and Nova Scotia, with a maximum 3-km water-depth at the end of rifting (if synrift sediments and salt deposits are removed). Because IB, MES and AF were moving together in the east-southeast direction with respect to NA during the rifting (Figure 21), a similar elongated depression was created between IB and NA, south of the barrier which connected GB and FC plates, but only minor extension took place along the Newfoundland-Gibraltar FZ (Figure 42). Thus, the two deep elongated depressions were connected by a very shallow sea (a few tens of meters deep), which followed the Newfoundland-Gibraltar FZ.

Figure 21 shows, from chrons ECMA to BSMA, the MES motion with respect to NA occurred in the southeast direction, creating a significant elongated depression along the Newfoundland-Gibraltar FZ. On chron BSMA paleo-geographic map (Figure 43), such an elongated depression exists along the whole Newfoundland-Gibraltar FZ, connecting not only the elongated central and north Atlantic oceans but also the central Atlantic to the ancient Tethys.

Pre-rift configuration: Late Triassic (Norian/Rhaetian limit, about 203 Ma)

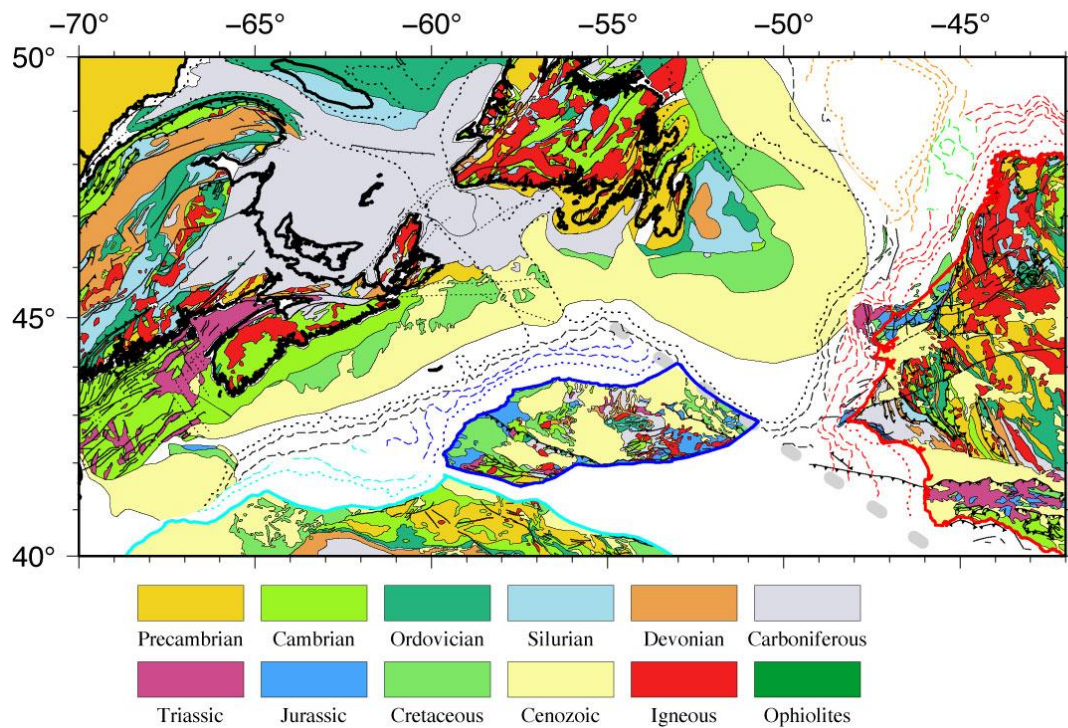


Figure 41: Pre-rift late Triassic geologic map on kinematic reconstruction at the Norian/Rhaetian limit (203 Ma).

Paleogeography of Early Jurassic (Sinemurian–Toarcian)

ECMA reconstruction (end of rifting) (Sinemurian/Pliensbachian limit, 190 Ma)

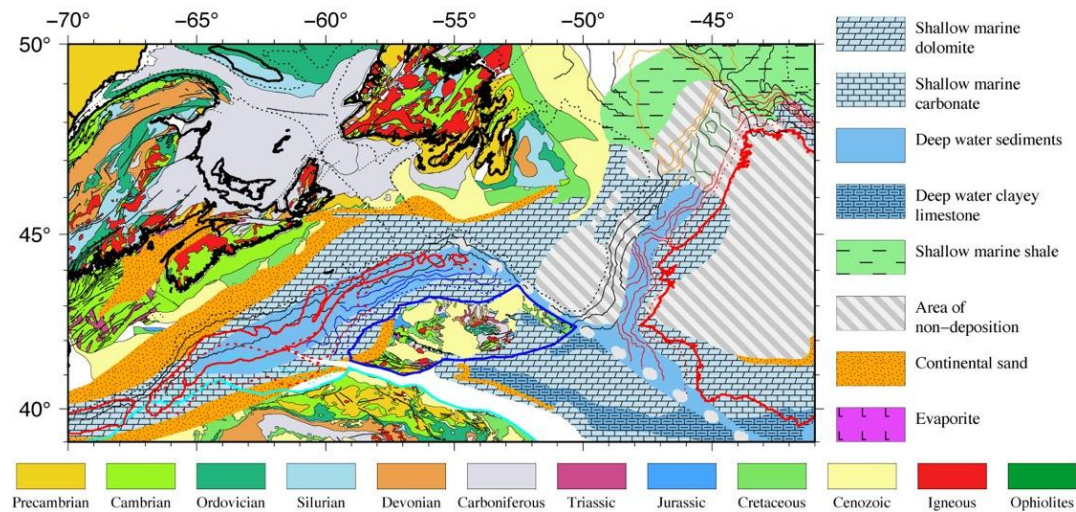


Figure 42: Sinemurian-Toarcian paleo-geographic map on kinematic reconstruction at chron ECMA (Sinemurian/Pliensbachian limit, 190 Ma).

Paleogeography of Middle Jurassic (Bajocian–Bathonian)

BSMA reconstruction (Middle Bajocian, 170 Ma)

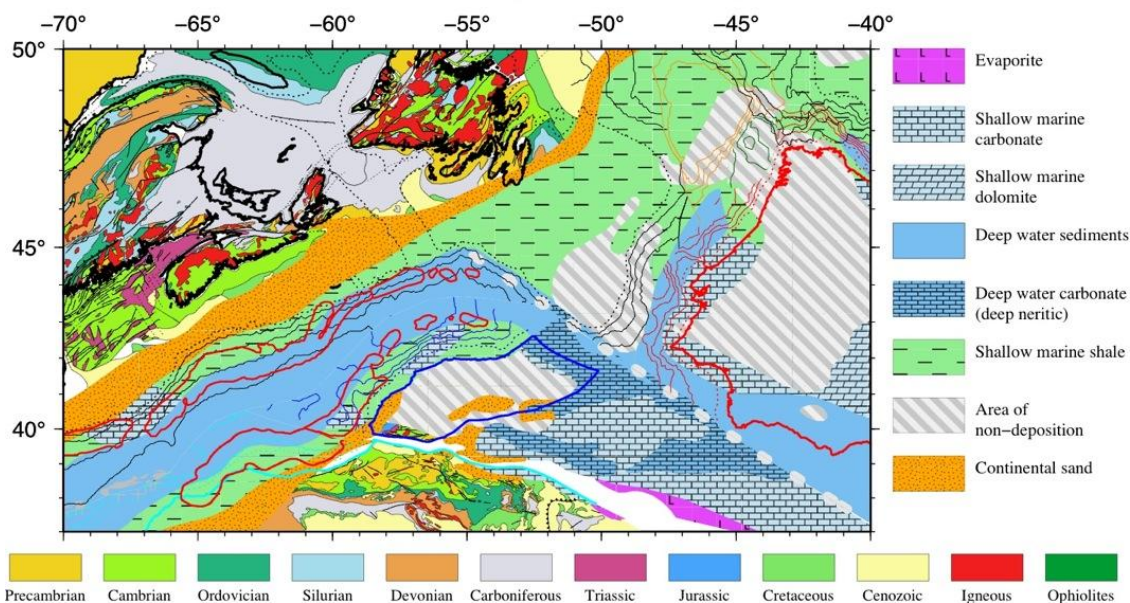


Figure 43: Bajocian-Bathonian paleo-geographic map on kinematic reconstruction at chron BSMA (middle Bajocian, 170 Ma).

Paleogeography of Late Jurassic (Oxfordian–Portlandian)

M22 reconstruction (Tithonian, 150 Ma)

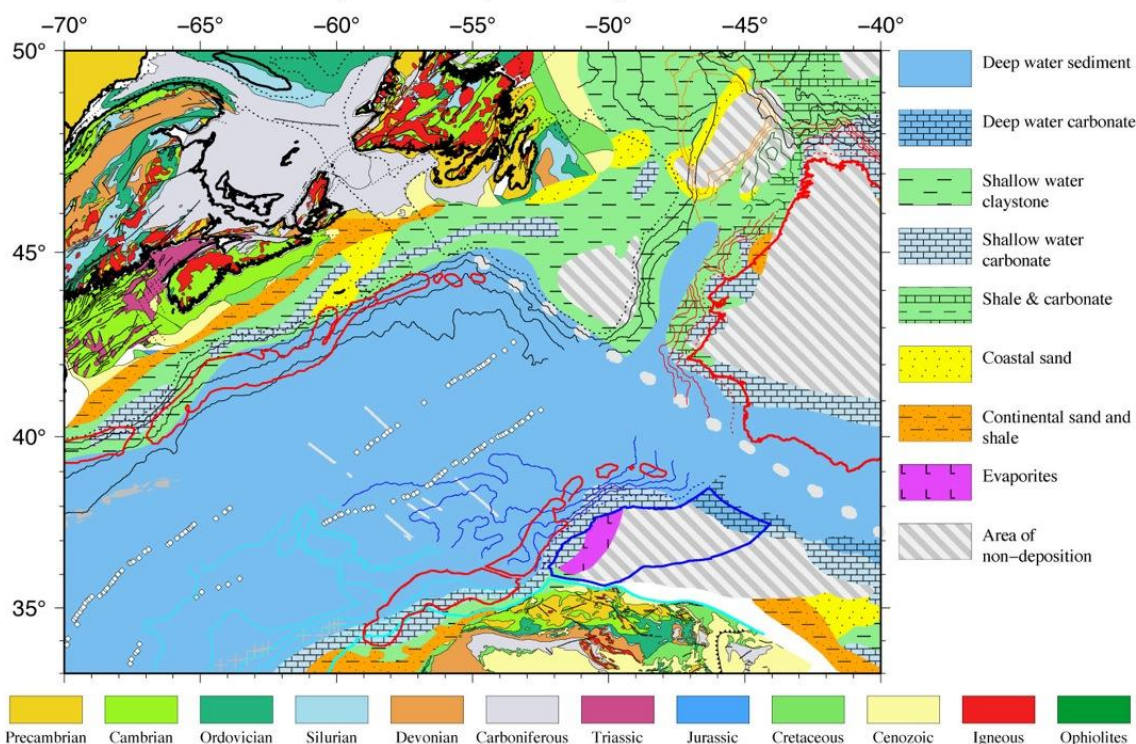


Figure 44: Oxfordian-Portlandian paleo-geographic map on kinematic reconstruction at chron M22 (middle Tithonian, 150 Ma).

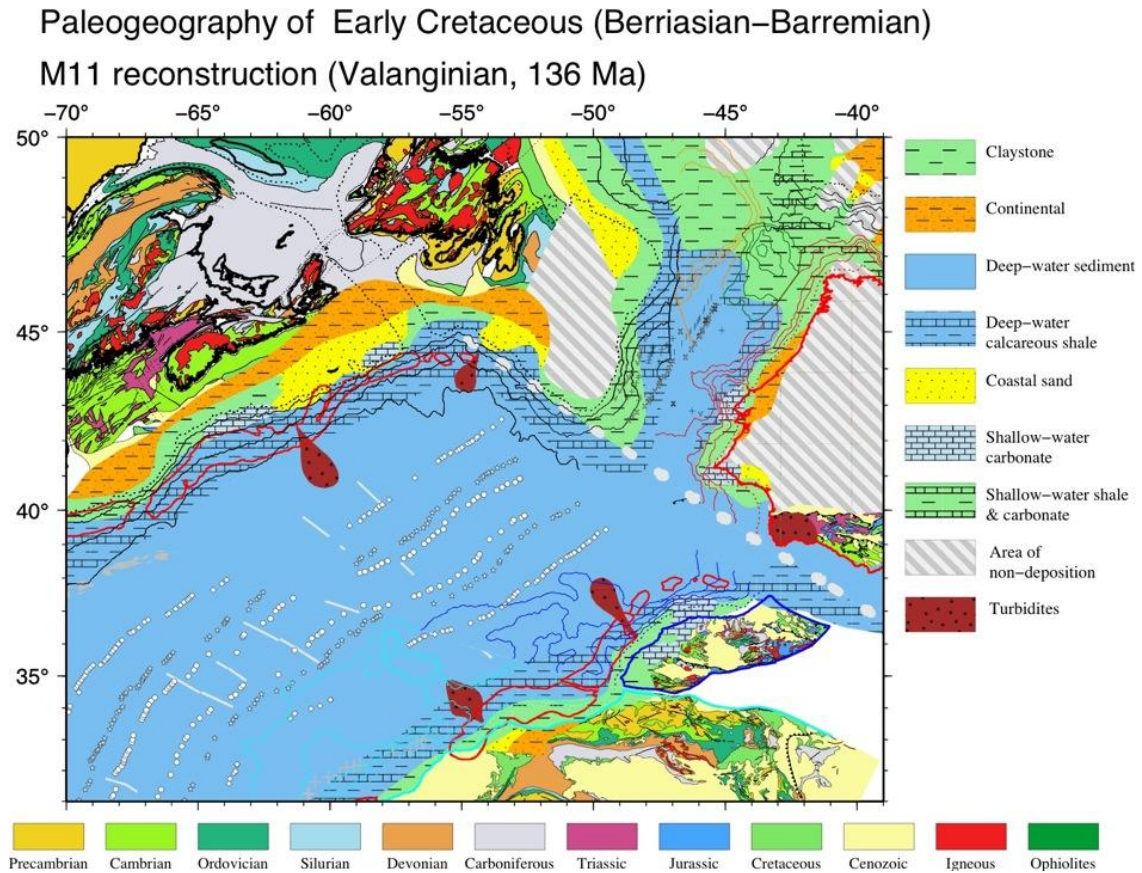


Figure 45: Berriasian-Barremian paleo-geographic map on kinematic reconstruction at chron M11 (Valanginian, 136 Ma).

Paleogeography of Middle Cretaceous (Aptian–Albian)
M0 reconstruction (Late Barremian/Early Aptian, 125 Ma)

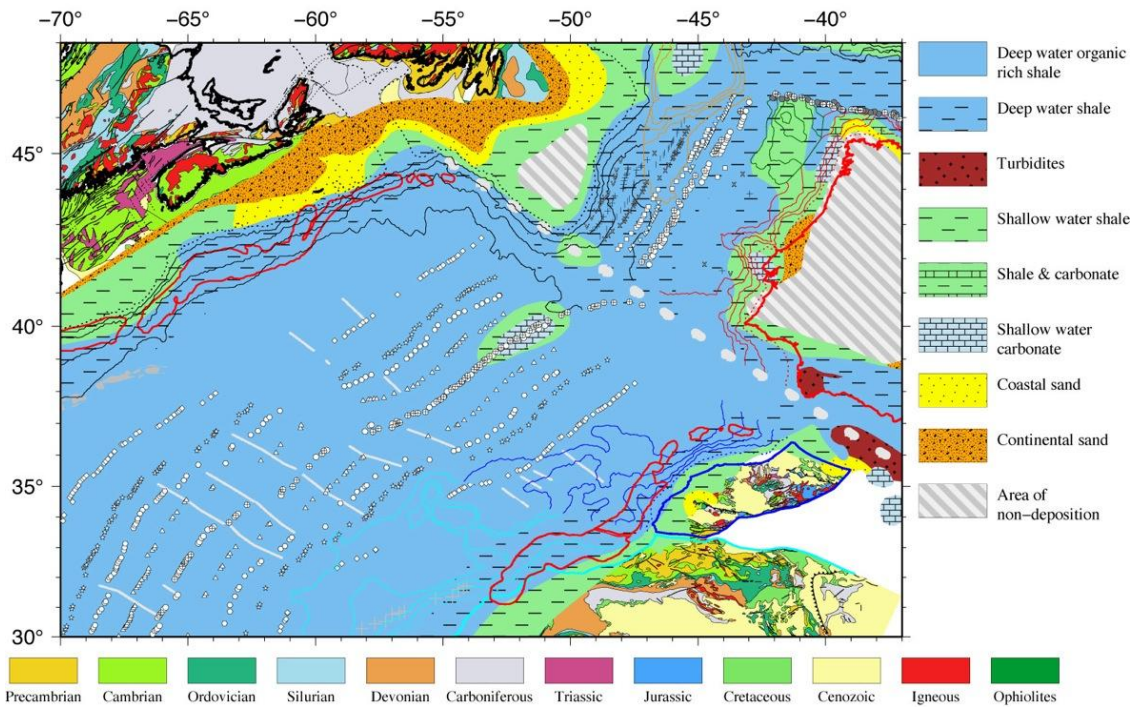


Figure 46: Aptian-Albian paleo-geographic map on kinematic reconstruction at chron M0 (late Barremian/early Aptian, 125 Ma).

Paleogeography of Late Cretaceous (Cenomanian–Danian)
C34 reconstruction (Santonian, 83.5 Ma)

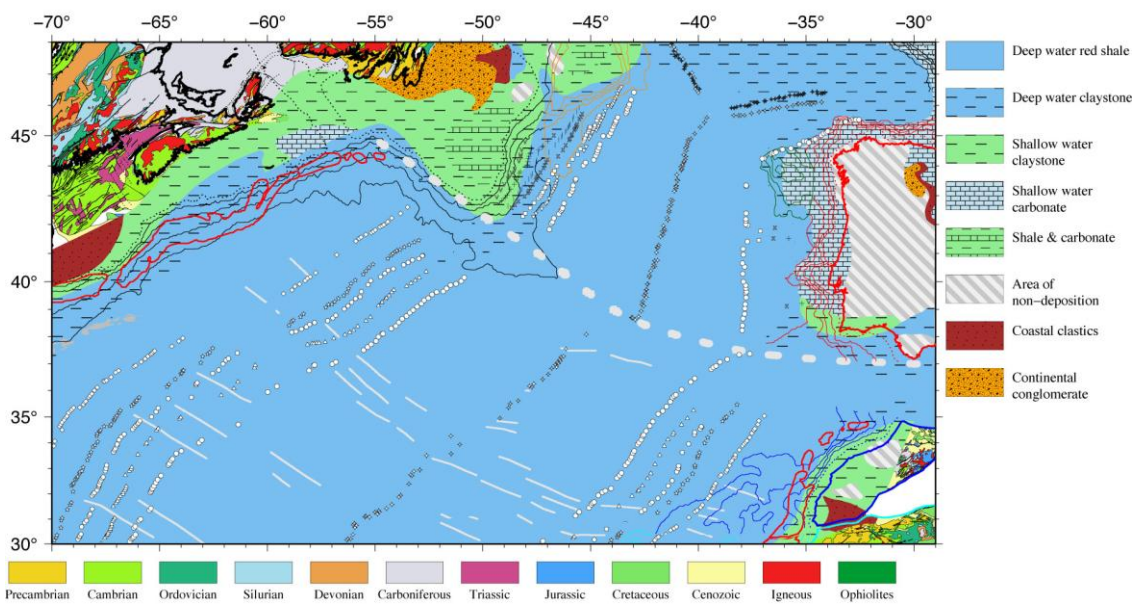


Figure 47: Cenomanian-Danian paleo-geographic map on kinematic reconstruction at chron C34 (Santonian, 83.5 Ma).

3. Conclusions

The SIMAR04 wide-angle and refraction line has been re-interpreted simultaneously with the coincident and adjacent high-quality MCS lines and the new findings concerning the trends of the northern prolongation of the ECMA and WACMA. The western limit of the Moroccan thinned continental crust is located between OBH09 and 10. Based on the shape of ECMA and WACMA, on the presence of salt in the domain located between OBH10 and 13 and on the absence of an autochthonous salt domain of similar shape on the Nova Scotia margin, refraction velocities have been interpreted as a portion of Nova Scotia thinned continental crust intruded by volcanics and transferred on the Moroccan side at chron ECMA. The domain located west of OBH13 is interpreted as oceanic crust abnormally thick due to the vicinity of Coral Patch Seamount. Further south and west of WACMA, sonobuoy data show that the domain consists in normal oceanic crust. Thus, the absence of serpentinized mantle on the Moroccan side suggests that, at the end of formation of the 90-km wide lower crustal high velocity body identified on OETR2009, SMART01 and SMART02 wide-angle lines, an eastward ridge jump occurred, leaving the whole high velocity body on the NA side. Consequently, the dipping reflectors identified in the upper part of the Moroccan oceanic crust are considered as mid-Jurassic in age and not as SDR's formed during the synrift period.

From the pre-rift situation to M0, the Labails et al. (2010) MES and AF/NA rotation parameters have been adopted. The detailed IB/NA kinematic work, including the role of GB and FC has been undertaken for periods older than chron M0. During the rifting period and early Jurassic, IB was attached to MES and then attached to NA from chron BSMA to M22. The resulting paleo-geographic maps shows that salt deposited in two elongated bathymetric depressions formed during the rifting period (late Triassic to chron ECMA) between Nova Scotia and Morocco and between IB and NA south of the GB-FC continental dam. Central Atlantic and north Atlantic waters were connected by a shallow sea located along the Newfoundland-Gibraltar FZ. After the end of salt deposition, this narrow bathymetric depression became deeper from chrons ECMA to BSMA, connecting the central and north Atlantic deep basins not only together but also with the ancient Tethys ocean.

Acknowledgments: Sonya Delher provided updated magnetic grids off Nova Scotia with integrated FUGRO data and off Morocco as well as the results of forward magnetic anomalies of ECMA along the four Nova Scotia refraction lines. Bernard Colletta from Beicip showed us numerous documents which allow us to better understand the general structural context of the Nova Scotia offshore. Dave Brown gave us access to the tremendous number of publications available on the Nova Scotia margin. Dave Roberts and Matt Luheshi always stimulated crucial discussions within the project and related to the geological context.

References

- Albertz, M., C. Beaumont, J. W. Shimeld, S. J. Ings, and S. Gradmann (2010), An investigation of salt tectonic structural styles in the Scotian Basin, offshore Atlantic Canada: 1. Comparison of observations with geometrically simple numerical models, *Tectonics*, 29, TC4017.
- Amante, C., and B. W. Eakins (2009), ETOPO1 1 Arc-Minute Global Relief Model: Procedures, Data Sources and Analysis, 19 p.

- Bown, J. W., and R. S. White (1995), Effect of finite extension rate on melt generation at rifted continental margins, *Journal of Geophysical Research*, *100*, 18,011-018,029.
- Bullock, A. D., and T. A. Minshull (2005), From continental extension to seafloor spreading: Crustal structure of the Goban Spur rifted margin, southwest of the UK, *Geophys. J. Int.*, *163*, 527-546.
- Christensen, N. I., and W. D. Mooney (1995), Seismic velocity structure and composition of the continental crust: A global view, *Journal of Geophysical Research*, *100*, 9761-9788.
- Contrucci, I., F. Klingelhoefer, J. Perrot, R. Bartolome, M.-A. Gutscher, M. Sahabi, J.-A. Malod, and J.-P. Réhault (2004), The crustal structure of the NW Moroccan continental margin from wide-angle and refraction data, *Geophysical Journal International*, *159*, 117-128.
- Davison, I., and P. Dailly (2010), Salt tectonics in the Cap Boujdour area, Aaiun Basin, NW Africa, *Marine and Petroleum Geology*, *27*, 435-441.
- Dehler, S. A. (2010), Initial rifting and break-up between Nova Scotia and Morocco: An examination of new geophysical data and models, paper presented at Central and north Atlantic conjugate margins conference, <http://metododirecto.pt/CM2010>, Lisboa.
- Dick, H. J. B., J. Lin, and H. Schouten (2003), An ultraslow-spreading class of ocean ridge, *Nature*, *426*, 405-412.
- Edwards, A., P. , P. Moir, and K. Coflin (2000), Structure and isopach maps of the Jeanne d'Arc Basin, Grand Banks, Newfoundland, *Geological Survey of Canada, GSC Open File 3755*.
- Funck, T., J. R. Hopper, H. C. Larsen, K. E. Loudon, B. E. Tucholke, and S. Holbrook (2004), Crustal structure of the ocean-continent transition at Flemish Cap: Seismic refraction results, *J. Geophys. Res.*, *108*(B11), 2531, doi:2510.1029/2003JB002434.
- Geological Map of North America, first edition, 1:5,000,000 (2005), edited by J. C. Reed, Jr., J. O. Wheeler, and B. E. Tucholke, U.S. Geological Survey Data Series 424.
- Gradstein, F. M., Jansa, L. F., Srivastava, S. P., Williamson, M. A., Bonham-Carter, G. and Stam, B. (1990), Aspects of North Atlantic paleo-oceanography, Chapter 8 in *Geology of the Continental Margin of Eastern Canada*, edited by M. J. Keen and G. L. Williams, Geological Survey of Canada, Geology of Canada, n°2, pp. 351-389 (also Geological Society of America, the Geology of North America, v. I-1).
- Hafid, M., G. Tari, D. Bouhadioui, L. El Moussaid, H. Echarfaoui, A. Ait Salem, M. Nahim, and M. Dakki (2008), Atlantic basins, in *Continental evolution: The geology of Morocco, Lecture notes in Earth Sciences*, edited by A. Michard, pp. 303-329, Springer-Verlag, Berlin, Heidelberg.
- Holik, J. S., P. D. Rabinowitz, and J. A. Austin (1991), Effects of Canary hotspot volcanism on structure of oceanic crust off Morocco, *Journal of Geophysical Research*, *96*, 12,039-012,067.
- Jokat, W., O. Ritzmann, M. C. Schmidt-Aursch, S. Drachev, S. Gauger, and J. Snow (2003), Geophysical evidence for reduced melt production on the Arctic ultraslow Gakkel mid-ocean ridge, *Nature*, *423*, 962-965.
- Klingelhoefer, F., L. Géli, L. Matias, N. Steinsland, and J. Mohr (2000), Crustal structure of a super-slow spreading centre: A seismic refraction study of Mohns Ridge, 72°N, *Geophysical Journal International*, *141*, 509-526.
- Klitgord, K. D., and H. Schouten (1986), Plate Kinematics of the Central Atlantic, in *The geology of the north Atlantic*, edited by P. R. Vogt and B. E. Tucholke, pp. 351-378, Geological Society of America, Boulder, CO.
- Labails, C., J.-L. Olivet, D. Aslanian, and W. R. Roest (2010), An alternative early opening scenario for the Central Atlantic Ocean, *Earth Planet. Sci. Lett.*, *297*, 355-368.

- Louden, K. E., J. C. Osler, S. P. Srivastava, and C. E. Keen (1996), Formation of oceanic crust at slow spreading rates: New constraints from an extinct spreading center in the Labrador Sea, *Geology*, *24*, 771-774.
- Maillard, A., J. Malod, E. Thiébot, F. Klingelhoefer, and J.-P. Réhault (2006), Imaging a lithospheric detachment at the continent-ocean crustal transition off Morocco, *Earth Planet. Sci. Lett.*, *241*, 686-698.
- Makris, J., K. Nunn, D. Roberts, and M. Luheshi (2010), A crust and basin study of the Nova Scotia margin and its ocean transition based on densely spaced ocean bottom seismic observations, paper presented at Central and north Atlantic conjugate margins conference, <http://metododirecto.pt/CM2010>, Lisboa.
- Matias, H., W. Mohriak, P. Menezes, F. Sandnes, V. C. F. Barbosa, L. Matias, and F. Santos (2005), Salt distribution and morphology in the offshore Algarve Basin, *25th annual Bob F. Perkins Research Conference: Petroleum systems of divergent continental margin basins, GCS-SEPM 2005*, 481-509.
- Maus, S., et al. (2009), EMAG2: A 2 – arc min resolution Earth Magnetic Anomaly Grid compiled from satellite, airborne, and marine magnetic measurements, *Geochem. Geophys. Geosyst.*, *10*, Q08005, doi:10.1029/2009GC002471.
- Nemcok, M., C. Stuart, M. P. Segall, R. B. Allen, C. Christensen, S. A. Hermeston, and I. Davison (2005), Structural development of southern Morocco: Interaction of tectonics and deposition *25th annual Bob F. Perkins Research Conference: Petroleum systems of divergent continental margin basins, GCS-SEPM 2005*, 151-202.
- Ogg, J. G., G. Ogg, and F. M. Gradstein (2008), *The Concise Geologic Time scale*, 150 pp., Cambridge University Press.
- Ranero, C. S., and M. Pérez-Gussinyé (2010), Sequential faulting explains the asymmetry and extension discrepancy of conjugate margins *Nature*, *468*, 294-300.
- Roeser, H. A., C. Steiner, B. Schreckenberger, and M. Block (2002), Structural development of the Jurassic Magnetic Quiet Zone off Morocco and identification of Middle Jurassic magnetic lineations, *J. Geophys. Res.*, *107*.
- Roest, W., J. J. Danobeitia, J. Verhoef, and B. J. Collette (1992), Magnetic anomalies in the Canary Basin and the Mesozoic evolution of the Central North Atlantic, *Marine Geophysical Researches*, *14*, 1-24.
- Royer, J. Y., R. D. Müller, L. M. Gahagan, L. A. Lawver, C. L. Mayes, D. Nürnberg, and J. G. Sclater (1992), A global isochron chart, Technical Rep. 117, 38 pp., University of Texas Institute for Geophysics, Austin, Texas.
- Russell, S. M., and R. B. Whitmarsh (2003), Magmatism at the west Iberia non-volcanic rifted continental margin: Evidence from analyses of magnetic anomalies, *Geophysical Journal International*, *154*, 706-730.
- Sahabi, M., D. Aslanian, and J.-L. Olivet (2004), A new starting point for the history of the central Atlantic, *Comptes Rendus Geoscience*, *336*, 1041-1052.
- Schettino, A., and E. Turco (2009), Breakup of Pangaea and plate kinematics of the central Atlantic and Atlas regions, *Geophysical Journal International*, *178*, 1078-1097.
- Sibuet, J.-C., S. Srivastava, and G. Manatschal (2007a), Exhumed mantle-forming transitional crust in the Newfoundland-Iberia rift and associated magnetic anomalies, *Journal of Geophysical Research*, *112*, B06105, doi:10.1029/2005JB003856, 2007.

- Sibuet, J.-C., S. P. Srivastava, M. Enachescu, and G. Karner (2007b), Early Cretaceous motion of Flemish Cap with respect to North America: Implications on the formation of Orphan Basin and S-E Flemish Cap/Galicia Bank conjugate margins, in *Imaging, Mapping and Modelling Continental Lithosphere Extension and Breakup*, edited by G. D. Karner, et al., pp. 63–76, Geological Society of London, Special Publications, DOI: 10.1144/SP282.4 0305-8719/07/\$15.00, London.
- Srivastava, S., J. Verhoef, and R. Macnab (1988), Results from a detailed aeromagnetic survey across the northeast Newfoundland margin, Part 2: Early opening of the north Atlantic between the British Isles and Newfoundland, *Marine and Petroleum Geology*, 5, 324-337.
- Srivastava, S., and J. Verhoef (1992), Evolution of Mesozoic sedimentary basins around the north Central Atlantic: a preliminary plate kinematic solution, in *Basins on the Atlantic seaboard: Petroleum geology, sedimentology and basin evolution*, edited by J. Parnell, pp. 397-420, Geological Society, Special publications, London.
- Srivastava, S., J.-C. Sibuet, S. Cande, W. R. Roest, and I. R. Reid (2000), Magnetic evidence for slow seafloor spreading during the formation of the Newfoundland and Iberian margins, *Earth and Planetary Science Letters*, 182, 61-76.
- Srivastava, S. P., W. R. Roest, L. C. Kovacs, H. Schouten, and K. Klitgord (1990), Iberian plate kinematics: A jumping plate boundary between Eurasia and Africa, *Nature*, 344, 756-759.
- Structural Map of the North Atlantic Ocean, first edition, 1:20 000 000 (2008), CGMW/UNESCO.
- Tari, G., and J. Molnar (2005), Correlation of syn-rift structures between Morocco and Nova Scotia, Canada 25th annual Bob F. Perkins Research Conference: Petroleum systems of divergent continental margin basins, *GCS-SEPM 2005*, 132-150.
- The 1:5 Million International Geological Map of Europe and Adjacent Areas (2005), 1:5,000,000 scale, edited by Bundesanstalt für Geowissenschaften und Rohstoffe (BGR), Hannover.
- Thinon, I., L. Matias, J.-P. Réhault, A. Hirn, L. Fidalgo-Gonzalez, and F. Avedik (2003), Deep structure of the Armorican basin (Bay of Biscay): A review of Norgasis seismic reflection and refraction data, *Journal of the Geological Society of London*, 160, 99-116.
- Tucholke, B. E., and J.-C. Sibuet (2007), Leg 210 synthesis: tectonic, magmatic, and sedimentary evolution of the Newfoundland-Iberia rift, in *Proceedings of the Ocean Drilling Program, Scientific Results, 210*, edited by B. E. Tucholke, et al., pp. 1-56, Ocean Drilling Program, College Station, TX.
- Tucholke, B. E., and R. B. Whitmarsh (2011), The Newfoundland-Iberia conjugate rifted margins, in *Principles of Phanerozoic regional geology*, edited by A. W. Bally and D. G. Roberts, p. in press.
- Verhoef, J., R. Macnab, and Project Team (1996), Compilation of magnetic data in the Arctic and north Atlantic oceans, *Bedford Institute of Oceanography unpublished report*, 1-13.
- Vogt, P. R., C. N. Anderson, and D. R. Bracey (1971), Mesozoic magnetic anomalies, sea-floor spreading, and geomagnetic reversals in the southwestern north Atlantic, *Journal of Geophysical Research*, 76, 4796-4823.
- Wade, J. A., and B. C. MacLean (1990), The geology of the southeastern margin of Canada, in *Geology of North America*, edited by M. J. M.J. Keen and G. L. Williams, pp. 167-238, Geological Society of America, Boulder.
- Wessel, P., and W. H. F. Smith (1998), New, improved version of Generic Mapping Tools released, *EOS trans. AGU*, 79, 579.

- White, R. S., D. McKenzie, and K. O'Nions (1992), Oceanic crustal thickness from seismic measurements and rare earth element inversions, *Journal of Geophysical Research*, 97, 19,683-19,715.
- Whitmarsh, R. B., P. Miles, J.-C. Sibuet, and V. Louvel (1996), Geological and geophysical implications of deep-tow magnetometer observations near ODP Sites 897, 898, 899, 900 and 901 on the west Iberia continental margin, in *Proc. ODP, Scientific Results*, edited by D. S. Sawyer, et al., pp. 665-674, College Station, TX (Ocean Drilling Program).
- Whitmarsh, R. B., G. Manatschal, and T. A. Minshull (2001), Evolution of magma-poor continental margins from rifting to seafloor spreading, *Nature*, 413, 150-154.
- Wu, Y., K. E. Loudon, T. Funck, H. R. Jackson, and S. A. Dehler (2006), Crustal structure of the central Nova Scotia margin off Eastern Canada, *Journal of Geophysical Research*, 111, 878-906.

Annex: Methodology used for the construction of kinematic, salt distribution, magnetic and paleo-geographic maps

A Origin of the data

The 200, 1000 to 4000 m **isobaths** are extracted from the ETOPO5, 5-minutes-gridded dataset (<http://www.ngdc.noaa.gov/mgg/global/relief/ETOPO5/>). The coastline itself comes from the "intermediate resolution" coastline (World Vector Shoreline) provided by the GMT package (Wessel and Smith, 1998).

The **magnetic picks** are digitized from different documents. Chron C34 picks are extracted from the Structural Map of the North Atlantic (2008). The outlines of ECMA and WACMA, BSMA and its African equivalent, as well as the M25-M0 sequence in the central Atlantic ocean are taken from Labails et al. (2010). Chrons M21 to M0 between Iberia and Grand Banks and chrons M0 between Iberia and Europe are from Sibuet et al. (2007a).

The **fracture zones** in the central Atlantic ocean are digitized from Labails et al. (2010). The location of the Newfoundland-Azores-Gibraltar fracture zone (thick light-gray dotted line) takes account of the northward continuation of the ECMA / WACMA.

The maps of **magnetic anomalies** are built using:

- the 1-minute grid of Verhoef et al. (1996) for most of the Atlantic ocean (default filling).
- the 2-minute EMAG2 grid of Maus et al. (2009) for the whole African plate and the onshore Meseta plate.
- the FUGRO grid provided by S. Dehler (personal communication, 2010) ranges from longitudes -67° to -54° and latitudes 40° to 47° and locally masks Verhoef's grid.
- an updated grid provided by S. Dehler off Morocco (personal communication, 2010) covers the offshore part of the Meseta plate.

The distribution of **salt** along the margins is a compilation of:

- Nova Scotia margin: Albertz et al. (2010), Wade and McLean (1990), Sahabi et al. (2004), Labails et al. (2010) and B. Colletta (personal communication, 2010).
- Grand Banks: Wade and McLean (1990), Edwards et al. (2000), Sahabi et al. (2004) and Labails et al. (2010).

- Moroccan margin: Tari and Molnar (2005), Hafid et al. (2008), Maillard et al. (2006), Sahabi et al. (2004), Labails et al. (2010) and Nemrock et al. (2005).
- Iberian margins : Davison and Dailly (2010) and Matias et al. (2000).

The **paleo-oceanography** and **paleo-facies** at chrons ECMA, BSMA, M22, M11, M0 and C34 are digitized from figure 8.3 of Gradstein et al. (1990).

The **geological maps** covering the onshore plates are digitized from:

- the Geological Map of North America (2005) for the North America plate.
- the 1:5 Million International geological map of Europe and adjacent areas (2005) for the Iberia, Meseta and Africa plates.

B Making of the kinematic reconstruction maps

The GMT package (Wessel and Smith, 1998) has been used throughout this study to plot the different maps.

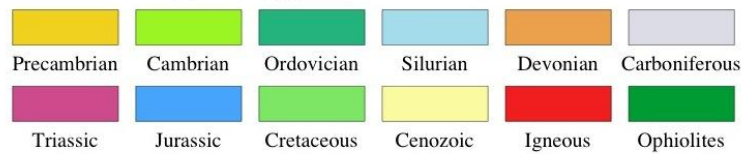
The Mercator projection is used for all the maps.

The rotation of the geological objects is performed using the program *rot_xyz* (Royer et al., 1992), modified to deal with geodetic latitudes.

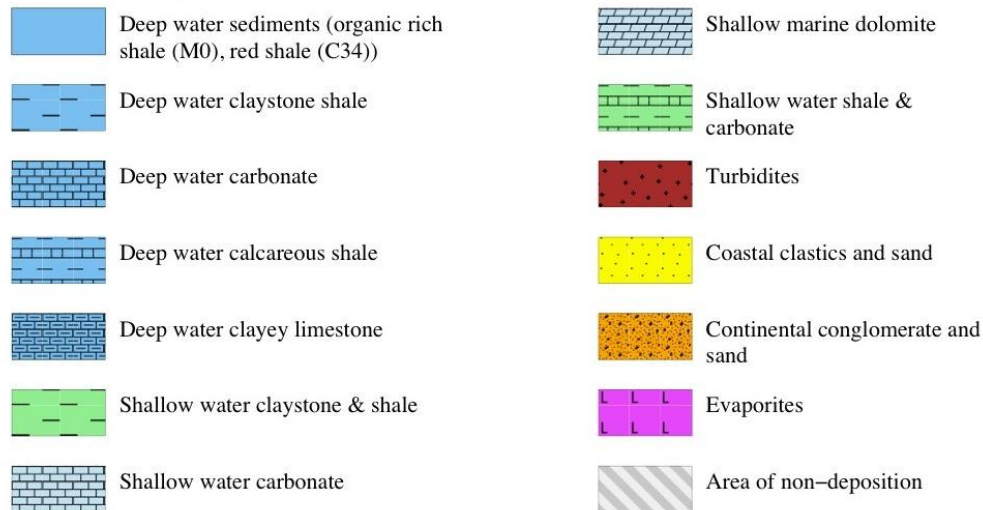
To preserve the accuracy of reconstructions, the paleo-facies digitized from the Gradstein et al. (1990) plates have been first rotated back to present position using *ad hoc* rotation parameters, before to be rotated with the specific parameters for the desired reconstruction. Eventually, minor editings have been performed to insure the continuity of structures and facies.

To facilitate the reading of the maps, Figure 48 presents the whole set of symbols and color codes used to represent the geology, paleo-facies, salt distribution and magnetic anomalies.

Onshore geology

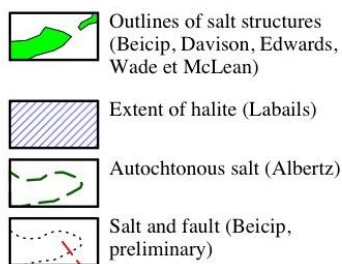


Offshore paleo facies

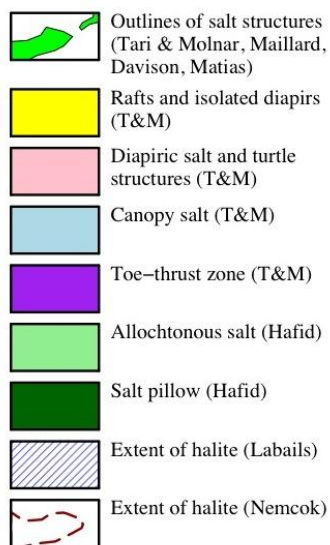


Salt distribution

North America



Africa, Meseta and Iberia



Magnetic anomalies

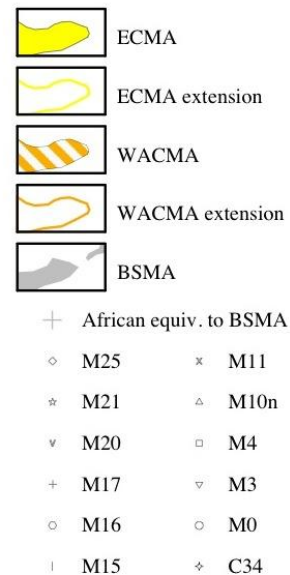


Figure 48: Symbols used in the kinematic, magnetic, salt distribution and paleo-geographic maps.